GENETICS, 2024, 227(1), iyae040
https://doi.org/10.1093/genetics/iyae040
Advance Access Publication Date: 20 March 2024
Multiparental Populations

Naturally segregating genetic variants contribute to thermal tolerance in a *Drosophila melanogaster* model system

Patricka A. Williams-Simon [1,*] Camille Oster,[2,8] Jordyn A. Moaton,[3,8] Ronel Ghidey,[4] Enoch Ng'oma [5]
Kevin M. Middleton [6] Elizabeth G. King [7,*]

[1]Department of Biology, University of Pennsylvania, 433 S University Ave., 226 Leidy Laboratories, Philadelphia, PA 19104, USA
[2]Ash Creek Forest Management, 2796 SE 73rd Ave., Hillsboro, OR 97123, USA
[3]2035 W Wellington Ave., Chicago, IL 60618, USA
[4]ECHO Data Analysis Center, Johns Hopkins Bloomberg School of Public Health, 504 Cathedral St., Baltimore, MD 2120, USA
[5]Division of Biology, University of Missouri, 226 Tucker Hall, Columbia, MO 65211, USA
[6]Division of Biology, University of Missouri, 222 Tucker Hall, Columbia, MO 65211, USA
[7]Division of Biology, University of Missouri, 401 Tucker Hall, Columbia, MO 65211, USA
[8]Present address: Division of Biology, University of Missouri, 401 Tucker Hall, Columbia, MO 65211, USA

*Corresponding author: Department of Biology, University of Pennsylvania, 433 S University Ave., 226 Leidy Laboratories, Philadelphia, PA 19104, USA.
Email: patwi@sas.upenn.edu, patrickaw21@gmail.com; *Corresponding author: Division of Biology, University of Missouri, 401 Tucker Hall, Columbia, MO 65211, USA.
Email: kingeg@umsystem.edu

Thermal tolerance is a fundamental physiological complex trait for survival in many species. For example, everyday tasks such as foraging, finding a mate, and avoiding predation are highly dependent on how well an organism can tolerate extreme temperatures. Understanding the general architecture of the natural variants within the genes that control this trait is of high importance if we want to better comprehend thermal physiology. Here, we take a multipronged approach to further dissect the genetic architecture that controls thermal tolerance in natural populations using the Drosophila Synthetic Population Resource as a model system. First, we used quantitative genetics and Quantitative Trait Loci mapping to identify major effect regions within the genome that influences thermal tolerance, then integrated RNA-sequencing to identify differences in gene expression, and lastly, we used the RNAi system to (1) alter tissue-specific gene expression and (2) functionally validate our findings. This powerful integration of approaches not only allows for the identification of the genetic basis of thermal tolerance but also the physiology of thermal tolerance in a natural population, which ultimately elucidates thermal tolerance through a fitness-associated lens.

Keywords: QTL; thermal tolerance; DSPR; RNA-seq; gene expression; RNAi; complex traits

Introduction

Thermal tolerance is a complex physiological and behavioral trait that determines the survivability of many individuals and, ultimately populations. Temperature regulates and plays a critical role in a wide range of processes from cellular functions—action potentials and enzymatic reactions (Schulte *et al.* 2011; Yu *et al.* 2012; Dowd *et al.* 2015)—to more systematic evolutionary processes like migration and population growth (Frazier *et al.* 2006; Sunday *et al.* 2012) and ultimately fitness (Angilletta 2009). Populations experiencing different temperature environments have evolved different physiological adaptations, which often lead to different thermal limits among populations (Jørgensen *et al.* 2019). However, like many other complex traits, identifying the genetic variants driving thermal adaptation has been challenging. Therefore, a model system allowing for a comprehensive understanding of the genetic architecture underlying thermal tolerance would significantly advance our understanding of the proximate mechanisms determining thermal limits.

Many empirical studies—both in model and non-model systems—demonstrate the importance of understanding the mechanisms contributing to thermal tolerance, including in coral (Dixon *et al.* 2015), fish (Schulte *et al.* 2011; Anttila *et al.* 2013; Grinder *et al.* 2020), fruit flies (Overgaard *et al.* 2008; Bozinovic *et al.* 2016), birds (Nord and Nilsson 2011; DuRant *et al.* 2012, 2013), frogs (Pintanel *et al.* 2019; Díaz-Ricaurte *et al.* 2021), and lizards (Angilletta, Hill, *et al.* 2002). The ability to tolerate extreme temperatures is essential for ectotherms (Huey and Berrigan 2001; Angilletta, Niewiarowski, *et al.* 2002; Frazier *et al.* 2006; Hoffmann 2010; Sunday *et al.* 2011; Gunderson and Stillman 2015) because their body temperature tracks the ambient temperature to a greater degree than endotherms. *Drosophila* species have been used extensively as a research model because of their worldwide distribution and vastly different thermal environments and preferences (MacLean, Sørensen, *et al.* 2019). *Drosophila melanogaster*, in particular, has been used for decades to study these traits in laboratory and field settings (James *et al.* 1997; Hoffmann *et al.* 2003; Kristensen *et al.* 2008; Bergland *et al.*

Received on 11 July 2023; accepted on 26 February 2024

2014; Ørsted et al. 2019; Machado et al. 2021; Rudman et al. 2022). For example, within a natural environment, Machado et al. (2021) demonstrated the effects of seasonal temperature shifts in allele frequencies of fruit flies, suggesting that short-term temperature changes can lead to rapid changes in allele frequencies. While these studies have been imperative in elucidating how ectotherms adapt to temperature changes and how the genome responds to such changes, there is still a lack of complete knowledge about the specific genetic mechanisms underpinning thermal tolerance.

Identifying the causative mechanisms at play in highly complex, multifaceted traits like thermal tolerance remains very challenging. Genetic mapping approaches, designed to identify loci associated with the naturally occurring variation in a trait continue to improve and have led to the discovery of many associations for thermal tolerance in fruit flies (Morgan and Mackay 2006; Vermeulen et al. 2008a, 2008b; Rand et al. 2010; Rolandi et al. 2018) and other systems including coral, fish, pigs, and cattle (Perry et al. 2001; Everett and Seeb 2014; Dixon et al. 2015; Kim et al. 2018; Matz et al. 2018; Cheruiyot et al. 2021). However, mapping approaches lack the resolution to identify single genes on their own (Mackay 2001). More recently researchers have been pairing mapping approaches with transcriptomics to identify candidate genes that influence complex traits (Cubillos et al. 2017; Highfill et al. 2017; Wen et al. 2019; Williams-Simon et al. 2019; Lecheta et al. 2020; Ng'oma et al. 2020), which was first introduced by Wayne and McIntyre (2002). While it is critically important to validate candidate genes that have been identified to be associated with complex traits, it has been a daunting task, and therefore few genetic studies of complex traits have definitively identified causal variants (Ding et al. 2016; Highfill et al. 2017; Gaspar et al. 2020). Approaches integrating several methods including multiparent mapping for high power and resolution, transcriptomics, and functional genomics provide a promising approach that moves beyond simply mapping loci toward identifying the key genes involved in complex traits. Here, we leverage the combined strengths of Quantitative Trait Loci (QTL) mapping, transcriptomics, and functional genetics to elucidate the genetic architecture of thermal tolerance using a large set of recombinant inbred lines (RILs) from the *Drosophila* Synthetic Population Resource (DSPR) multiparental population (King, Macdonald, et al. 2012; King, Merkes, et al. 2012). We measured over 700 RILs for thermal tolerance and identified multiple QTLs, including 1 large effect QTL. We then performed RNA-seq to identify several candidate genes that are located within our QTLs and performed validation studies using classical genetics. Through this multifaceted approach, we identified novel candidate genes associated with the critically important trait, thermal tolerance.

Methods

DSPR and fly husbandry

We used the DSPR, which is a multiparental mapping population for the *D. melanogaster* system (King, Macdonald, et al. 2012; King, Merkes, et al. 2012; Long et al. 2014); (http://FlyRILs.org). The DSPR consists of approximately 1,600 8-way RILs, with 2 populations (pA and pB), which consist of approximately 800 RILs each. Each population was created by crossing a set of 8 founder lines, with 7 unique founders to each population and 1 that is shared—AB8. Each RIL is a mosaic of the 15 founders (parental) lines, which have been fully re-sequenced, and the RILs have been genotyped at over 10,000 SNPs. This structure makes genomic analysis of this population more feasible, because of the ability to be able to track entire haplotypes (King, Macdonald, et al. 2012). To generate the RILs, the founders were mixed en masse for 50 generations to create a synthetic population, with 2 major goals—first to generate high genetic diversity, then for high mapping resolution. The population was then inbred for another 25 generations to create stable recombinant inbred lines (King, Merkes, et al. 2012). Within each of the pA and pB populations, 2 separate synthetic populations were maintained (e.g. pA1 and pA2) for the crossing phase before the creation of the RILs. We phenotyped 741 RILs in population A, scoring thermal tolerance for each line (Fig. 1a).

We raised stock RILs at 18°C and 60% relative humidity on a standard fruit fly diet (Supplementary Table 1) with live yeast added to the top of the food after it cooled. Maintenance of our stock lines occurred at 18°C because this made it more feasible to maintain the high number of RILs we needed for this experiment. Two weeks before phenotyping for thermal tolerance, approximately 10 female and 6 male flies were placed into a flask (Fisher Scientific, cat. no.: AS-355) of food and maintained at 25°C for 1 week to allow for mating and egg laying. After the first week (7 days, post-oviposition), we removed all the adults (parental generation) from the flasks first to ensure that there was no mixing of generations and second to control for density while making sure we had sufficient adults for phenotyping. After 2 weeks (14 days post-oviposition), we anesthetized adult flies on ice for no more than 10 min and selected 60–80 female flies for the thermal tolerance assay. We then divided flies equally between 2 separate vials of food and allowed them to recover for at least 24 h before the phenotyping assay. The age range for all individuals we assayed was 15–22 days post-oviposition (5–13 days post-eclosion). This age range allowed us to obtain and assay a large number of flies per line. Throughout this experiment, we only measured mated female flies to keep the experiment at a reasonable size. Successfully mapping a complex trait such as thermal tolerance requires assaying a massive number of individuals and measuring both sexes would effectively double the size of the experiment. Thus, while we anticipate sex effects, we were unable to include both sexes at the scale that would be needed.

Measuring thermal tolerance in the DSPR

We measured thermal tolerance using a thermally-controlled and highly sensitive apparatus known as the "heat box" (Wustmann et al. 1996). Within the heat box, there are 16 individual chambers, which allows for concurrent testing of flies. In each chamber, temperatures are set at 24°C for the first 30 s for acclimation, then immediately shift to 41°C for 9.5 min for a total of 10 min (Wustmann et al. 1996; Zars 2001). Every chamber has a temperature sensor that reports the temperature of that chamber in real time. The temperature change within each chamber is rapid and takes 4 s to reflect 41°C (Wustmann et al. 1996). Additionally, we independently confirmed that the chambers reflected the temperature at the given time by inserting a thermocouple in each chamber periodically. While 10 min is a short period of time, the vast majority of RILs are incapacitated within this timeframe with fewer than 1% of RILs remaining active for the full 10 min. We assayed the RILs in a randomized order, limiting the number of flies assayed on a single day from a single RIL up to 27 individuals total (2 groups in the heat box), to ensure each RIL was assayed over multiple days, however, we ran several RILs on any given day. For each RIL, we assayed a minimum of 30 individuals. We also measured the founder lines for thermal tolerance, following the same experimental design as we did for the RILs, except for AB8, which did not thrive in our hands, and thus, we do not have

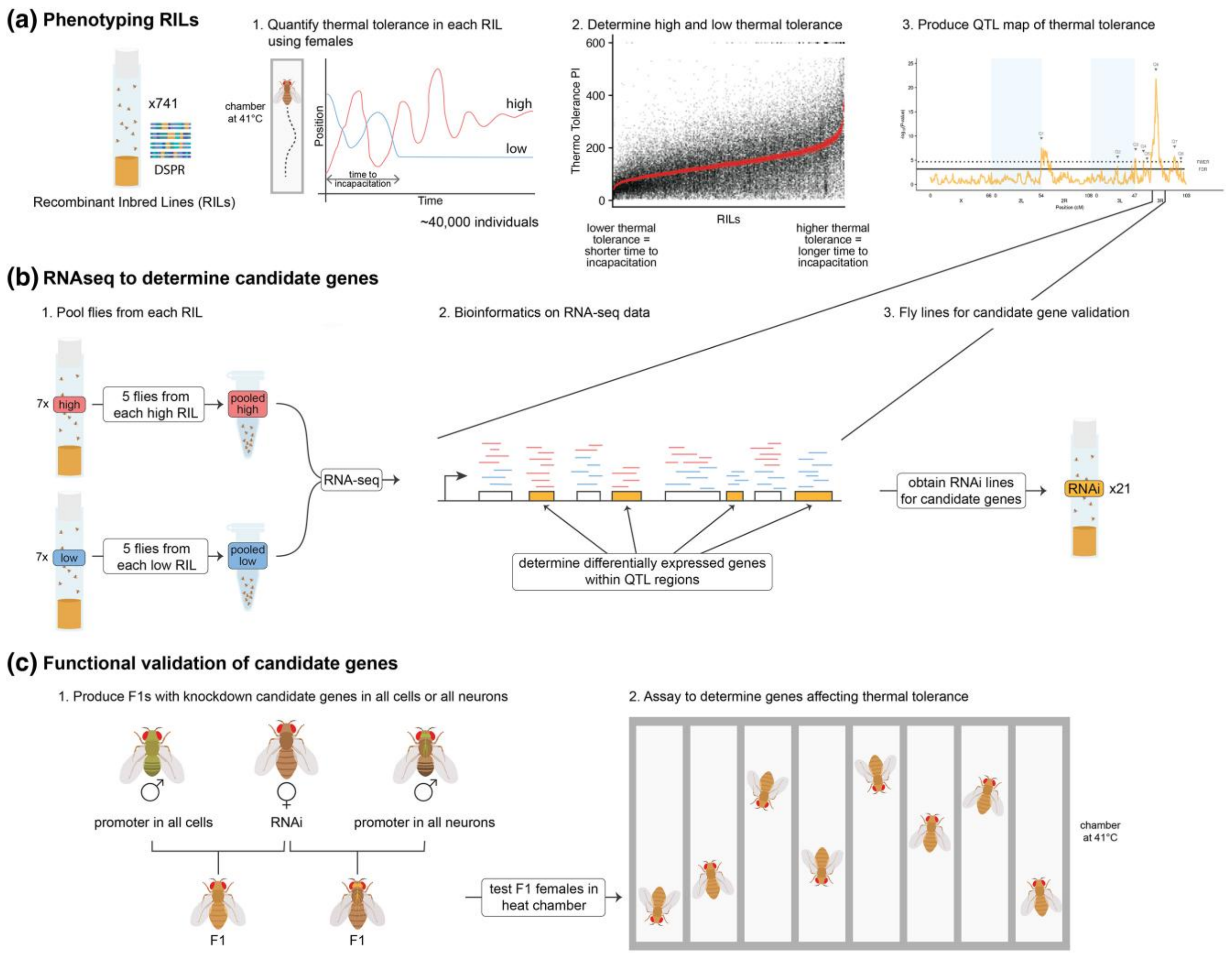

Fig. 1. Schematic of the experimental design. a) Phenotyping and QTL mapping using the DSPR RILs, b) RNA-seq and differential expression analysis, and c) using RNAi lines for functional validation of candidate genes within the QTL interval.

an estimate for that line. We measured a total of 424 individuals from the founding populations, with an average of 61 individuals per founder (range: 48–67).

We define thermal tolerance as the amount of time it takes before a fly becomes incapacitated for at least 60 s. We used a custom R script to automate scoring incapacitation based on the criteria defined above (i.e. no activity for 60 s). The heat box contains an infrared system for monitoring each fly's position within the chamber. We used a sliding window to assess the variance in position in 60 s intervals and scored a fly as incapacitated when this variance was below a threshold value indicating no substantial movement within that interval. This approach has the advantage of applying purely objective, defined criteria to scoring incapacitation. However, it is important to confirm the program produced the correct results. We validated our script by comparing over 5,000 visually hand-scored incapacitation scores to our automated-scored values (Supplementary Fig. 1). These scores are highly correlated ($r = 0.88$), and manual inspection of discrepancies between the hand-scored and automated-scored values revealed the automated values to be more accurate and consistent for our defined criteria for incapacitation.

QTL mapping and heritability

We performed a genome scan on 741 RILs using a custom R script as described in Williams-Simon *et al.* (2019). We used the average incapacitation times from each RIL as phenotype and applied the Haley–Knott regression (Haley and Knott 1992). This statistical approach regresses each phenotypic average on the 8 founder haplotype probabilities (Broman and Sen 2009; King, Macdonald, *et al.* 2012) by fitting the following model:

$$y_i = \sum_{j=1}^{7} p_{ij} b_{ij} + e_i,$$

where y_i is the phenotype (i.e. thermal tolerance) of the ith RIL, p_{ij} is the probability the ith RIL has the jth haplotype at the locus, b_{ij} is the vector of effects for the jth haplotype, and e_i is the vector of residuals (Broman and Sen 2009). Prior to performing this genome scan, we transformed the raw phenotypic data, using a square root transformation, which improved the normality distribution of the data to meet the assumptions of our statistical test. The DSPR RILs contain 2 subpopulations within each set of RILs, stemming from the synthetic populations being maintained en masse in 2 sets before the creation of the RILs (King, Macdonald, *et al.* 2012). Including subpopulations (pA1 and pA2) in the model did not affect the mapping results (Supplementary Fig. 2a). We also performed a second genome scan after correcting for our most significant QTL (Q5) and did not obtain any additional peaks (Supplementary Fig. 2b). We also performed local association mapping for our most significant QTL (Q5) by fitting a similar model with SNP probabilities rather than haplotype probabilities. We calculated these probabilities from the haplotype probabilities for each RIL at each position and the SNP genotypes in the founder lines.

To identify statistically significant QTLs, we used permutations to calculate both the false discovery rate (FDR) and the family-wise error rate (FWER). First, we permuted thermal tolerance along with place learning and place memory phenotypes (Williams-Simon *et al.* 2019), because we assayed all 3 of these phenotypes on the same individual fly during heat box the experiment. For context, we define place learning and memory as the ability of an individual fly to associate a side of the chamber between 2 different temperatures (aversive—41°C or preferred 24°C), and the remembering to avoid the side associated with the aversive temperature (Ostrowski *et al.* 2018), respectively. Second, we computed the number of false positive QTLs at a range of different significance thresholds. We removed any QTL that were within 2 cM of a more significant QTL to identify distinct QTLs. Then, we calculated the empirical false discovery rate (FDR, expected false positives/total positives) for each threshold and determined the threshold corresponding to a 5% FDR. We also calculated the threshold corresponding to a 5% family-wise error rate (FWER, the probability of 1 or more false positives experiment-wide) by determining the lowest *P*-value for each set of genome scans from each permutation and calculated the 95% quantile of the resulting set of *P*-values (Churchill and Doerge 1994). For each identified peak, we calculated the estimated effects of each haplotype at each QTL, the percent variance explained (PVE) by the QTL and the Bayesian credible interval (BCI), following the methods described previously for the DSPR (King, Macdonald, *et al.* 2012). If the BCI of 2 significant QTLs did not overlap, we considered these distinct QTLs.

We calculated broad-sense heritability ($H^2 = V_G/V_P$) of thermal tolerance by estimating the genetic and phenotypic variance and covariance from a linear mixed model *lme* and *VarCorr* functions in the *nlme* package (Pinheiro and Bates 2000; Pinheiro *et al.* 2023) followed by a jackknife, which allowed us to obtain standard errors of our estimate (Roff and Preziosi 1994; Roff 2008). The jackknife removes each observation once, the model is then fit, and the quantitative genetic parameter (i.e. heritability) is estimated and a pseudo value is calculated. Prior to fitting the model, we quantile-transformed the raw data to ensure normality. Thus, for our dataset of 741 RILs, each RIL is deleted, 1 at a time, to produce 741 pseudo values. Because the *lme* function uses restricted maximum likelihood, it is possible for the model to not converge. This occurred for 72 cases, thus, these pseudo values were not included in the calculation of our estimates. We also performed a model comparison using a likelihood ratio test to determine the significance of RIL (i.e. genotype). We compared the model fitting only the intercept to the model including RIL, fitting both via maximum likelihood such that model comparisons would be valid.

Structural variants analysis

Structural variants (SVs), for example, insertions, deletions, and transposable elements, contribute to the phenotypic variation in complex traits (Frazer *et al.* 2009; Eichler *et al.* 2010; Chakraborty *et al.* 2018). Chakraborty *et al.* (2019) used the DSPR to identify genome-wide SVs in both populations A and B, which we utilized to determine if there were any SVs located within the BCI of our most significant QTL (Q5). To ensure that we captured all the SVs located in the QTL region, we included any genes that had any portion within the BCI, even if the entire gene did not fall within the QTL BCI.

RNA-sequencing

We performed RNA-seq on mated female heads to determine differentially expressed genes between the top and bottom cohorts of thermal tolerance (Fig. 1b). It is important to note that in our design, we only used heads which allowed us to only focus on gene expression within a specific tissue type. There is physiological evidence that incapacitation in high temperatures results from failure in the central nervous system (Jørgensen *et al.* 2020), thus, we chose the head as the most logical tissue to focus on.

First, we selected 14 RILs from the high ($n = 7$) and low ($n = 7$) 5% cohorts after phenotyping the first 140 RILs and followed the same set-up protocol (see phenotyping section above). In total, we had 6 pooled samples consisting of 5 individual female heads from each of the 7 lines in the cohort. Thus, for each of the 6 samples, we pooled a total of 35 female heads in a single sample, with 5 heads from each RIL contributing to each sample. Adult female flies 14 days post-oviposition were flash-frozen in liquid nitrogen and stored at −80°C, until further processing. We used a narrower age range here, choosing flies at the same age that females were set up for phenotyping. In addition, we also took a different set of individuals from the same RILs and cycled them through an "incubation assay" for 1 min intervals at 41°C and 24°C (room temp) for a total of 6 min, and left control samples on the benchtop at a constant 24°C also for 6 min. Then, all the vials–from both experimental and control groups–were left on the benchtop at room temp for 3 h. To ensure: (1) flies were just incapacitated and not dead from heat stress, and (2) the gene expression changes had time to occur but also that there was minimal time to allow for gene expression turnover. Immediately after the 3 h, flies were flash-frozen in liquid nitrogen and stored at −80°C. For the incubator assay, all RILs were tested between 8 AM and 10 AM, to help reduce possible confounding effects that would affect gene expression. The samples were then freeze-dried overnight to prevent the degradation of RNA, using a lyophilizer (Labconco, cat. no.: 77550-00). Second, the samples were shipped to Rapid Genomics (Gainesville, FL) for transcriptome processing. The total RNA was extracted with Dynabeads mRNA direct kit from Life Technologies, mRNA was then fragmented and converted into double-stranded cDNA, followed by the standard proprietary library prep for 1 lane of Illumina HiSeq 3000 instrument to generate paired-end (PE) reads. The first 16 samples were PE 150 bp, while the remaining samples were PE 100 bp. Third, We analyzed the RNA-seq data using a bioinformatic pipeline, as described previously in Williams-Simon *et al.* (2019). Briefly, we trimmed the samples using the software *cutadapt* (Martin 2011), then ran a quality control test using *fastqc* (Leggett *et al.* 2010), which did not show any significant issues with the reads. We then used parts of the *Tuxedo* pipeline (Pertea *et al.* 2016) to align the reads against the *D. melanogaster* reference transcriptome (Ensembl Release Version: 84) using *HISAT2* (Kim *et al.* 2015) and *StringTie* (Pertea *et al.* 2015, 2016) assembled and quantified transcripts. To calculate the read count for each gene we used a *prepDE* Python script provided for this purpose (http://ccb.jhu.edu/software/stringtie/index.shtml?t=manual#deseq). The resulting dataset provided the input needed to use the *DESeq2* package (Love *et al.* 2014) to identify differentially expressed genes. We filtered out any zero count genes and performed surrogate variables analysis (SVA) on the normalized count data (Leek *et al.* 2012, 2019) to estimate any unknown batch effects. We identified 2 significant surrogate variables, which we included as terms in the models we fit along with our known batch effect (i.e. sampling day) in all following bioinformatics analyses. We then used the DESeq2 package (Love *et al.* 2014) to test for overall treatment effects and performed contrasts between pool (high and low cohorts), condition (temperature: 41°C or room temperature), and the interaction between pool and condition, identifying significantly differentially expressed genes for each. To estimate the differences in expression in each pool and condition, we used the function *lfcShrink*, which performs shrinkage on $\log_2$(fold changes). All $\log_2$(fold changes) reported here are the shrinkage estimated values using the "*normal*" estimator. We then used the contrasts to identify candidate genes that were differentially expressed between the different groups localized within the BCIs of the mapped QTLs (Q1–Q7).

RNAi lines and crossing design

Because the Q5 QTL indicated a very strong association with thermal tolerance and the BCI was fairly narrow, we further investigated the genes within this QTL using RNAi lines. We sourced the UAS-RNAi transgenic fly lines from the Transgenic RNAi Project (TRiP) from the Bloomington Drosophila Stock Center (BDSC; Perkins *et al.* 2015). BDSC reported that the TRiP RNAi lines might have a low dose of *Wolbachia pipientis*, therefore we treated the flies with tetracycline (Sigma-Aldrich, cat. no.: T4062-5G, batch: SLCF9393). We followed a tetracycline treatment protocol from Hoffmann *et al.* (1986). We incorporated 0.3 mg/mL final concentration of tetracycline into an agar base fly food recipe and allowed the flies to remain on that food for 2 generations flipping them onto new agar food after 2 weeks. One of the lines did not survive during the tetracycline treatment (BDSC stock no.: 63713). After the treatment, we switched the population back to our "normal" fly food recipe (Supplementary Table 1) and allowed the lines to re-acclimate to the food for 5 generations before beginning experiments. The TRiP collection did not have RNAi lines for all 21 genes in the Q5 interval. However, we obtained RNAi lines for 14 genes from the BDSC, some of which had more than 1 available RNAi line (Supplementary Table 2). We checked each UAS line for reports of off-target effects and did not identify any reported off-target effects (https://fgr.hms.harvard.edu/up-torr). In total, we screened 20 UAS-RNAi lines using 2 different promoters: (1) ubiquitously expressed using an *actin (Act5C-Gal4)* driver (BDSC–3954: *y1 w*; P{Act5C-GAL4}17bFO1/TM6B, Tb1*), and (2) pan neuronally expressed using *embryonic lethal abnormal vision* (*elav*) driver (BDSC–25750: *P{w[+mW.hs]=GawB}elav[C155]w[1118]; P{w[+mC]=UAS-Dcr-2.D}2*). All the UAS-RNAi lines were in either P2 (Chr 3) or P40 (Chr 2) background, which we used as controls for comparing thermal tolerance.

For each line, we placed adults from the parental stock in fresh vials and allowed them to mate. On day 3, we cleared the vials of all adults, then on days 9–12, we collected 3 males (Gal4) and 5 females (UAS-RNAi) to set up the cross to obtain Gal4-UAS-RNAi F_1 progeny. The *Act5C-Gal4* line has a tubby (*TM6B*, *tb1*) phenotypic marker, which we selected against at the pupae stage of development in the F1 because tubby is a pupae marker. Therefore, to make a fair comparison, we also transferred all lines on days 19–22 to control for transferring the tubby lines. On days 20–23, we anesthetized the flies using CO_2, collected 10 F_1 females (0–1 day post-oviposition), placed them in a new vial with food, and allowed at least 12 h of recovery time before measuring thermal tolerance.

Measuring thermal tolerance in RNAi lines

We measured the time it takes for individuals to become incapacitated in our RNAi crosses (Fig. 1c). Flies were placed individually into small clear cylinder tubes (5 mm diameter × 65 mm length; monitor tubes; TriKinetics, Inc., USA), which were plugged on both ends to prevent the flies from escaping. We placed the tubes onto a custom-milled aluminum plate (6.11 mm thick) with 34 individual slots (2.1 mm thick spaced 1.6 mm apart) matching the diameter of the fly tubes, allowing even heating throughout the tube. The aluminum plate is mounted to a Peltier-element based heating plate (PELT-PLATE; Sable Systems International, Inc., North Las Vegas, NV), which is connected to a controller, maintaining the plate at a constant temperature of 41°C. A temperature probe was also placed into a monitor tube for each run to monitor the accuracy of the temperature within the fly tubes relative to the PELT-PLATE.

We measured each cross in 3 batches of ∼10 individuals per run for a total of 10 min at 41°C. We deliberately designed systems for identifying when human errors occurred during testing, such as the plate not being aligned with the heat source, or the camera being out of alignment and dropped any samples where we identified an issue to ensure consistent measurements. Following this process, we had measurements for between 21 and 60 individuals for each cross. Before each trial, we confirmed that the aluminum plate was at ambient temperature before placing the monitor tubes into the wells. We randomized the assay order for the lines for the first replicate and kept that order for the second and third batches.

During each 10-min thermal tolerance trial, the entire set of flies was recorded using a Raspberry Pi High Quality Camera (12.3 MP) at 1 frame per second using a Raspberry Pi 4 Model B and custom Python code. Simultaneously, this script also recorded the timestamp, temperature reported by the PELT-PLATE, and temperature in the monitor tube measured via a thermocouple. Because the Raspberry Pi camera produces a highly distorted "fish-eye" image, we first de-warped the individual images via checkerboard calibration using 15 images covering the entire plate surface (Supplementary Fig. 3). The images were subsequently combined into a single movie for later analysis, both using routines in the OpenCV library (Bradski 2000).

Movies of the thermal tolerance trials were analyzed using DeepLabCut (version 2.2.3; Mathis *et al.* 2018; Nath *et al.* 2019) and custom Python scripts to enable batch processing of trials. Because each trial recorded the activity of many flies simultaneously, we needed to first split each composite video into a movie of a single fly's movements. The rigid nature of the aluminum thermal plate allowed for the automated extraction of video for individual flies. First, we located the 4 corners of the plate using a trained DeepLabCut model (Supplementary Fig. 4a). With coordinates of the 4 corners, we applied a second dewarping step, rotated the image so that the edges were normal to the frame, and cropped the image to the 4 corners using routines in the OpenCV library (Bradski 2000). Second, we leveraged the fixed coordinates of the fly tubes within the plate to subset each video into 34 separate videos, each with a single fly, no fly, or the thermocouple (Supplementary Fig. 4b). These videos were then processed using a second DeepLabCut model, which had been trained on 978 manually labeled frames from individual fly movies (1,000,000 training iterations; train error = 1.64 pixels; test error = 1.69 pixels; Supplementary Fig. 4c). This automated system was able to track 1,350 flies across ∼800,000 individual frames, yielding Cartesian (*x*, *y*) coordinates for each fly at each 1 s timestep. With these time and position data, we used an R script to automate identifying when individual flies were incapacitated using the same criteria described for the heat box.

To determine the effect of each RNAi cross on the incapacitation phenotype, we compared the UAS-Gal4-RNAi crosses and the background control cross by fitting separate ANOVAs for each RNAi line with the cross id as the predictor and incapacitation time as the response variable. We followed this model with planned post hoc comparisons using the *glht* function in the *multcomp* package (Hothorn *et al.* 2008), comparing each RNAi cross with the relevant matching background cross.

Validation of thermal tolerance phenotyping

Our mapping experiment used the heat box (see *Measuring thermal tolerance in the DSPR* section above) to track activity in individual flies in chambers lined individually with Peltier elements. We developed an alternative method for measuring incapacitation following this experiment for 2 reasons: (1) the heat box showed more variability than desired in the target temperature reached, and we identified instances where individual heat box chambers did not reach the desired temperature (these data were discarded from our dataset, see above), and (2) the heat box can measure, at most, 16 individuals at 1 time, limiting the speed we can perform assays. The heat plate method we developed, described above, resolved both issues, increasing the throughput of the assay and allowing for consistent assay temperatures with continuous monitoring. To confirm that our phenotyping methods are comparable, we measured a subpopulation of 39 RILs from those that were assayed in the heat box. We assayed these RILs in 2 biological replicates, assaying ∼60 individuals each time (range: 27 individuals to 72 individuals) for a set of RILs distributed across the range of thermal tolerance scores using the heat plate apparatus and methodology (Supplementary Fig. 5a). We observed shorter incapacitation times overall on the heat plate, which is expected given that the heat plate showed better consistency in reaching and maintaining the target temperature of 41°C than the heat box, but confirmed that the scores are correlated between the 2 methods ($r = 0.36$). We acknowledge that the correlation between the assays is not particularly high, and that there are differences between the 2 assays. For assaying thermal tolerance, the heat plate is more consistent, which is why we have moved to this method. In the heat box measurements, the same individual was first assayed for place learning and memory, resulting in individuals previously exposed to 41°C at varying durations as they learn (for more details, see section above and Williams-Simon *et al.* 2019). In addition, in the heat box, each chamber has a separate heating element, leading to small variations in the temperature in each, whereas the heating element in the heat plate assay is 1 block, which means the onset of the 41°C is uniform. Thus, while both assays give a proxy measurement for thermal tolerance, we believe these differences in the assays are driving the differences we see some differences between the 2 assays. As with the heat box, we validated our measurements by hand-scoring a set of actual videos of flies moving for incapacitation and examined a set of traced movies to confirm both the tracking performance and the programmatic scoring of incapacitation. We compared the human scores to the computer-generated scores, which had an overall positive correlation (Supplementary Fig. 5b; $r = 0.47$).

All data analyses were performed in R 4.2 and lower (Posit team 2023; R Core Team 2023), Python 3.9.0 (Van Rossum and Drake 2009), and DeepLabCut 2.2.3 (Mathis *et al.* 2018).

Results

Phenotypic distributions

We first quantified thermal tolerance in 741 RILs (39,392 individuals) in the DSPR using the heat box (Fig. 1a). We found a wide range of phenotypic variation with approximately a 15-fold range from 24 to 361 s between RILs with low and high average incapacitation times (Fig. 2). We expected thermal tolerance to show high variability among RILs because the original founding parents of the RILs were collected from different continental locations (King, Merkes, *et al.* 2012) with varying adaptation to different temperatures and it is also a characteristic complex trait. We also phenotyped the DSPR founder lines (A1, A2, …, A7) directly for thermal tolerance (Fig. 3b).

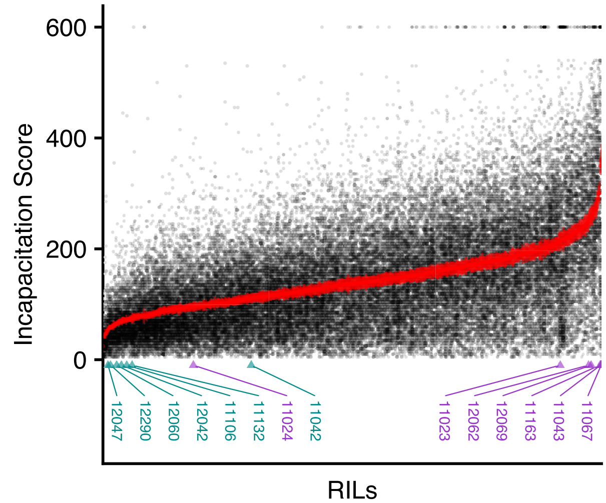

Fig. 2. Incapacitation scores for all individuals (>48,000) for the 741 DSPR RILs measured. Each point represents an individual fly's phenotype with points plotted with semi-transparency so overlap can be visualized as darker areas. The RILs are sorted on the x axis by their mean incapacitation score. The mean score ± 1 SE for each RIL is plotted from min to max. The ids of the 14 RILs used for RNA-seq are labeled on the x axis.

We estimated broad-sense heritability (H^2) for thermal tolerance in the RILs, which was $H^2 = 0.24$, 95% CI = 0.22–0.26. In addition, the effect of RIL ID on thermal tolerance was highly significant ($\chi_1^2 = 11, 232.13$, $P < 0.0001$), indicating that there is a genetic basis for thermal tolerance in the DSPR RILs.

QTL

We identified 7 QTLs (Q1–Q7; Fig. 3a; Table 1) at the 5% FDR and higher. Of those 7 QTLs, 5 reached or passed the FWER threshold, which is the more stringent threshold. Any significant QTLs are potential regions of the genome that influence thermal tolerance, with Q5 having the strongest association. For each significant QTL, we determined the region most likely to contain causative variants by obtaining a Bayesian credible interval (BCI; Manichaikul *et al.* 2006; Broman and Sen 2009). For Q5, the most significant QTL, the BCI is 20.93–21.09 on chromosome 3R. Therefore, for each of our significant QTL, we can estimate the founder (A1, A2, A3, A4, A5, A6, A7, and AB8) haplotypes' effect at the specific QTL location for thermal tolerance (Q5: Fig. 3c; all QTL: Supplementary Fig. 6). For example, at Q5, the set of RILs harboring the A5 haplotype at that location have the highest average incapacitation score, while those harboring the A4 haplotype have the lowest, though the means do not form 2 distinct groups, suggesting the potential for multiple causative variants in this interval.

We also performed local association mapping within the Q5 peak interval to identify which DSPR variants showed the strongest association with thermal tolerance. Given that we have complete genome sequences for all founder haplotypes and have

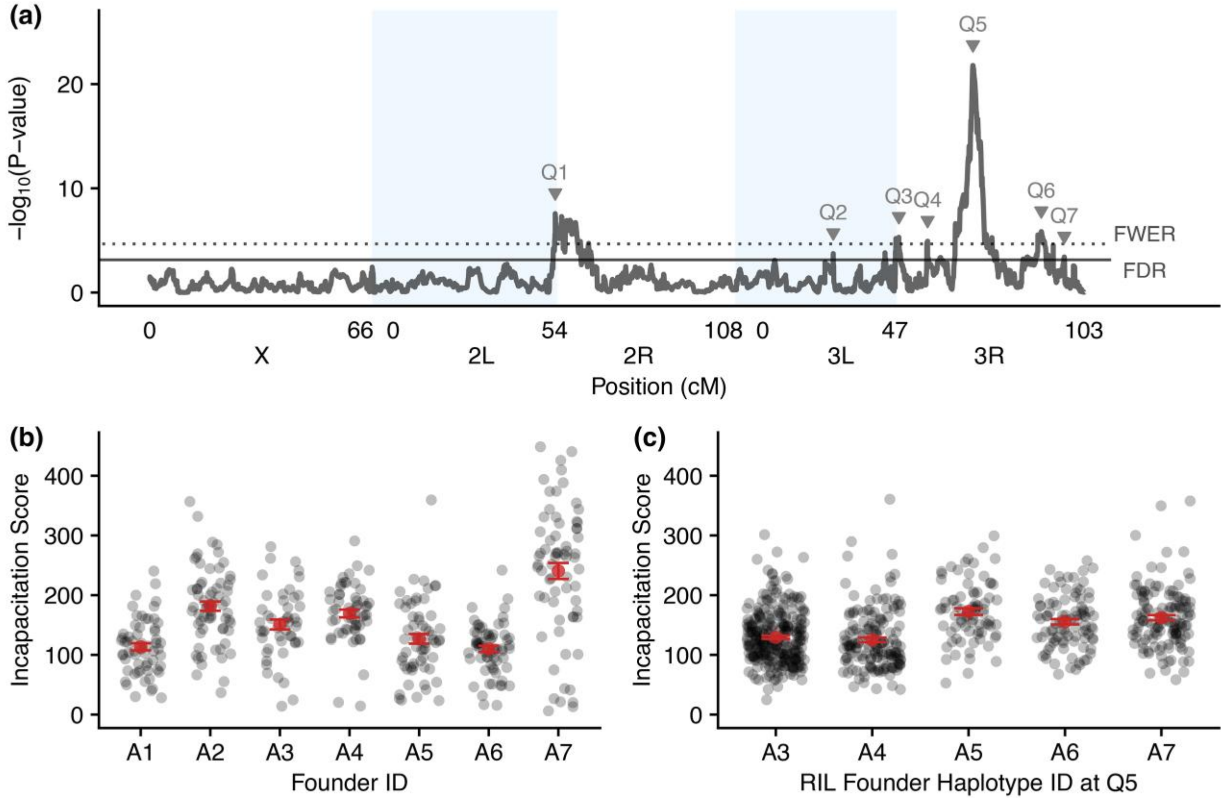

Fig. 3. Genome-wide scans. a) Genome scan for thermal tolerance in the DSPR RILs showing the $-\log_{10}$(P-value) vs position in the genome with different chromosome arms denoted by shaded boxes. Each QTL that reached at least the FDR threshold is labeled at the corresponding QTL peak. The FDR (solid line) and FWER (dotted line) thresholds are shown with horizontal lines. b) The raw incapacitation scores measured in the inbred founder lines. Each point represents an individual fly's phenotype with points plotted with semi-transparency so overlap can be visualized as darker areas. The mean score ± 1 SE for each founder line is plotted. c) The average incapacitation scores in the RILs with RILs separated by the founder haplotype they harbor at the Q6 location. Each point represents a RIL mean with points plotted with semi-transparency so overlap can be visualized as darker areas. The mean score ± 1 SE for the set of RILs harboring each founder haplotype at Q6.

Table 1. Details for all QTLs.

ID	Arm	Position (Mbp)	Lower (Mbp)	Upper (Mbp)	$-\log_{10}$(P-value)	PVE (%)
Q1	*2L*	20.11	2L:22.07	2R:8.69	7.57	6.4
Q2	*3L*	9.39	8.82	9.42	3.74	3.8
Q3	3R	8.02	5.53	8.28	5.30	4.9
Q4	3R	15.40	15.26	17.37	4.93	4.6
Q5	3R	20.98	20.93	21.09	21.79	14.9
Q6	3R	26.33	26.00	26.63	5.84	5.2
Q7	3R	28.94	26.97	30.40	3.41	3.6

inferred the haplotype identity for each RIL at each position, we can compute the probability a given RIL harbors a given SNP at each position. We can then use these probabilities in a linear model rather than the founder haplotype probabilities. This approach is most useful to identify the set of "in phase" SNPs that might correspond to a clear high vs low group, which would be suggestive of a single causative SNP underlying the QTL. However, in this case, and most cases in the DSPR, there is evidence for multiallelism (more than 1 causative SNP) with haplotypes not forming a clear high and low grouping (Supplementary Fig. 7), thus interpretation is more challenging. In addition, because haplotype probabilities do not change very much across the BCI region, the association mapping results will be similar for SNPs that share the same haplotype groupings (e.g. the set of SNPs unique to 1 founder will all have the same predictive power). As a result, there are significant SNPs located near all genes in the interval and thus this analysis does not narrow down our set of potential candidate genes.

RNA-seq and genome-wide expression patterns

We performed RNA-seq on a pooled set of mated female heads to identify differentially expressed genes between low and high cohorts of thermal tolerance performance, assaying expression at both room temperature and following exposure to high temperature. Thus, we obtained genome-wide expression profiles (Fig. 4) for 4 separate groups: thermal tolerance high performers at room temperature (H_RT), thermal tolerance low performers at room temperature (L_RT), thermal tolerance high performers after incubation (H_Incu), and thermal tolerance low performers after incubation (L_Incu).

First, to determine the level of genome-wide expression patterns in the different cohorts, we performed principal components analysis (PCA) on all samples using the expression matrix (Supplementary Fig. 8). PC1 explains 29% of the variance, while PC2 explains 22% of the variance. There is a clear separation between the samples incubated at high temperatures and those measured at room temperature. Both high- and low-performance pools following high-temperature exposure (Incu) cluster together, whereas there is a substantial separation between high and low pools (H and L) at room temperature (RT).

Next, we determined differences in gene expression patterns in the different cohorts (Fig. 4; Supplementary Fig. 8b). There were

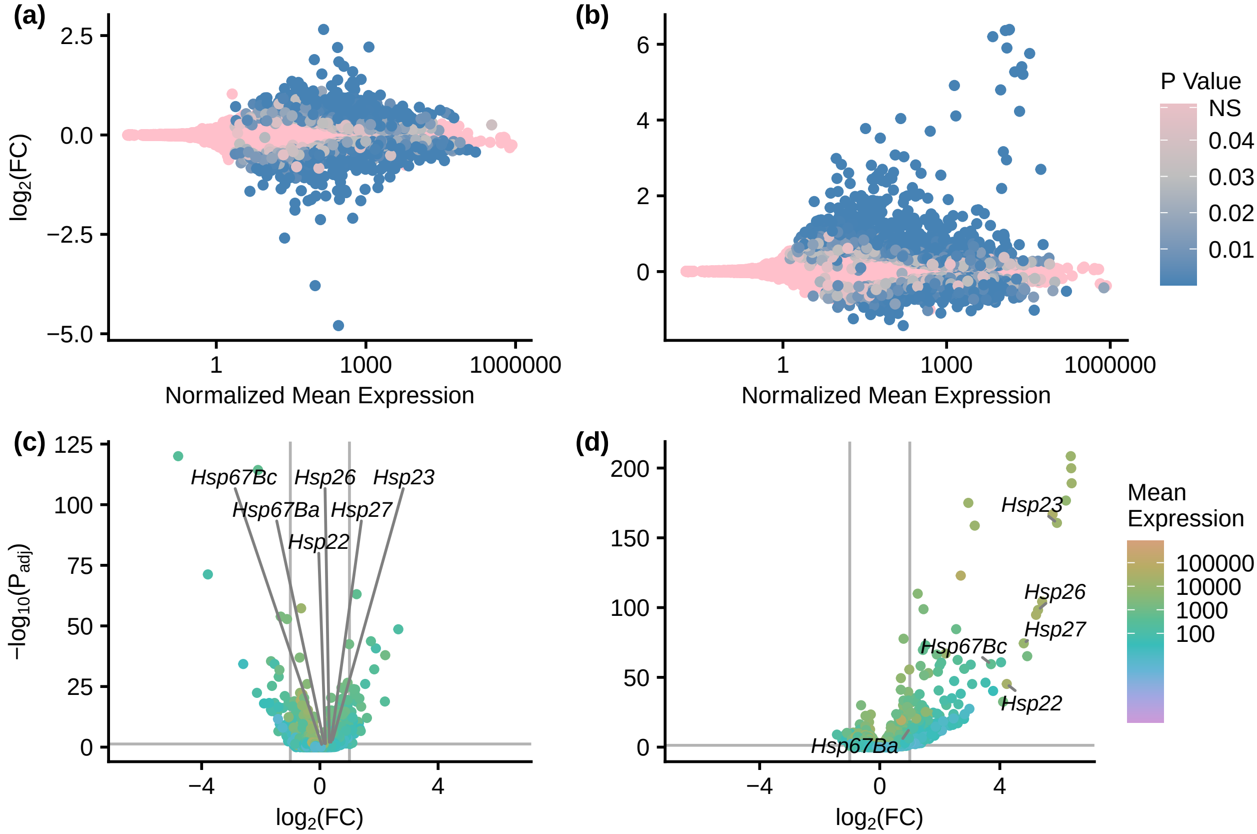

Fig. 4. Differential gene expression. a,b) MA plots showing $\log_2$(fold change) for the high vs low pools a) and the incubated vs room temperature pools b) vs the normalized mean expression value for each gene. Normalized mean expression is shown on a $\log_{10}$ scale. Genes are colored by *P*-value with nonsignificantly differentially expressed genes in pink and increasingly significant genes in darker shades of blue. c,d) $\log_2$(fold change) for the high vs low pools c) and the incubated vs room temperature pools d) vs $-\log_{10}$(adjusted *P*-value). The gradient of the points shows the normalized mean expression value of each gene. The *Hsp* genes that fall within Q2 are labeled on each plot.

2,642 genes that were differentially expressed between high vs low (pool) cohorts for thermal tolerance genome-wide. In this comparison, 1,215 genes had higher expression in the high pool and 1,427 had higher expression in the low pool (Fig. 4). Of those genes, 191 were located between our QTL's BCI (Q2 = 18; Q3 = 49; Q4 = 35; Q5 = 8; Q6 = 15; Q7 = 66; Supplementary Fig. 9), obviously, higher numbers of genes are located under the QTLs with wider BCIs. Q1 is excluded here because the BCI spans a centromere. In the incubated vs room temperature (condition) comparison, 2,862 genome-wide genes were differentially expressed between high and low cohorts for thermal tolerance. In this comparison, 1,608 genes had higher expression in the incubated condition and 1,254 had higher expression at room temperature. There were 256 genes differentially expressed within our QTL intervals (Q2 = 29; Q3 = 66; Q4 = 59; Q5 = 8; Q6 = 12; Q7 = 82; Supplementary Fig. 10).

We then wanted to examine if any Heat Shock Protein (HSP) genes within our QTL intervals were differentially expressed within the cohorts (pool or condition) because *Hsps* are characterized as genes important for thermal tolerance in fruit flies and other species (Krishnan *et al.* 1989; Sørensen *et al.* 2001; Pörtner 2002; Fangue *et al.* 2006; Lockwood *et al.* 2017). Within Q2, which is located on chromosome *3L*, there were 6 differentially expressed *Hsp* genes (*Hsp22*, *Hsp23*, *Hsp26*, *Hsp27*, *Hsp67Ba*, and *Hsp67Bc*) in the condition cohort, which has some consistency with work done by Freda *et al.* (2022), whereas only *Hsp23* was significant in the pool cohort.

Candidate genes in the Q5 region

Among our identified QTLs, Q5 was much more significant than the other peaks (Fig. 3a), indicating that this locus has a larger effect on thermal tolerance, and therefore we consider Q5 a QTL of high interest. Q5 is located on chromosome 3R there are 21 genes located within that BCI region (Supplementary Figs. 9d and 10d). Eight of the 21 genes were significantly differentially expressed between high and low pools at room temperature: *annexin B9* (*anxB9*), *cortactin* (*cortactin*), *dynein heavy chain* (*dhc93AB*), *malvolio* (*mvl*), *Na pump alpha subunit* (*α*), *rho GTPase activating protein* (*RhoGAP93B*), *CG31207*, and *CG7079*. We focused on differential expression based on standing expression in the low and high pools at room temperature because our thermal tolerance assay is short (10 min) and changes in gene expression in response to temperature would require longer timescales to impact the phenotype.

RNAi

In order to investigate the effect of differences in gene expression for genes within the Q5 interval on thermal tolerance we used the TRiP lines with knockdown expression of a particular gene. We quantified thermal tolerance in 20 UAS-RNAi mutant lines (1,969 individuals), representing 14 genes (Supplementary Table 2), which we crossed to Act-Gal4 (all cells) and elav-Gal4 (all neurons). We observed significant phenotypic effects on several of these crosses (Fig. 5; Supplementary Fig. 11; Supplementary Table 2), with the most common effect being a decrease in

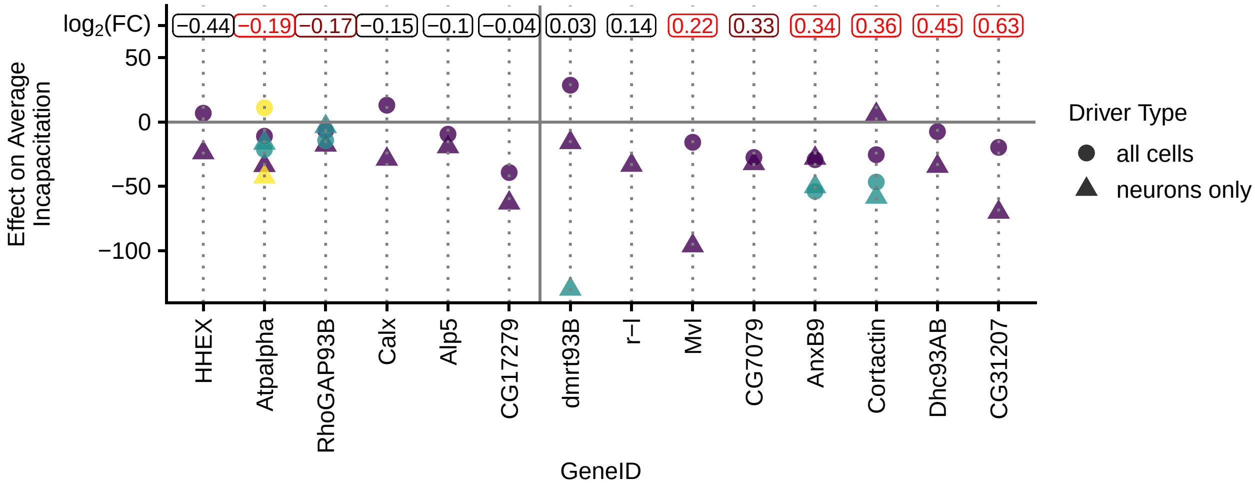

Fig. 5. Validation through functional genetics. The effect of RNAi knockdown for each assayed gene within the Q6 BCI. Plotted points show the difference between average incapacitation scores between each RNAi cross and the corresponding background cross for each gene within the Q6 BCI assayed. Negative numbers indicate the RNAi cross had a lower average incapacitation score than the matching background cross. Different shapes show drivers targeting different sets of tissues with circles representing the driver targeting all cells (ubiquitously expressed) and triangles showing the driver specific to neurons (pan-neuronal). Some genes had more than 1 RNAi line available so for those cases, there are two or more triangle or circle to represent the different RNAi lines. In some cases, all crosses for a particular driver—RNAi line combination was not successful and thus those are not plotted. Genes are ordered on the *x* axis by the degree of differential expression between pools of lines showing high vs low incapacitation. The $\log_2$(fold change) for each gene is displayed at the top of the plot with significantly differentially expressed genes shown in red (dark red = $0.01 < P < 0.05$; red = $P < 0.01$).

incapacitation time compared to the background cross. Adding this RNAi evidence to our existing data, we selected 5 genes (*anxB9*, *cortactin*, *Dhc93AB*, *Mvl*, and *CG31207*) as possible candidates, based on several lines of evidence.

First, we started with a list of all the genes that were located within the BCI for Q5 and that were also significantly differentially expressed in our RNA-seq dataset (Fig. 5; Supplementary Fig. 12). Second, we combined this list with the RNAi data, where we measured the changes in incapacitation compared to the background line when that particular gene was knocked down. We considered a gene worthy of further consideration if the direction of the RNAi effect was consistent with our RNA-seq results (e.g. a gene with higher expression in the high thermal tolerance group should show a decrease in thermal tolerance in the RNAi cross), this effect was significant for at least 1 cross for that focal gene, and there was overall consistency in the direction of the effect in the set of crosses for the gene. The 1 exception to this criterion is *Dhc93AB*, which we include because it was one of our most significantly differentially expressed genes and the phenotypic effect of the RNAi line was consistent with the expected effect, though this effect was not significant. The following genes met these criteria: *anxB9*, *cortactin*, *Dhc93AB*, *Mvl*, and *CG31207*, and the effects and significance for these genes are shown in Table 2. While not every RNAi cross associated with a given gene showed a statistically significant effect, there is general consistency in the direction of the effect for the genes in our candidate list across crosses.

Furthermore, we investigated if there were any SVs located within the DSPR founders with haplotypes located at the Q5 region, following the protocol of (Chakraborty *et al.* 2019). SVs are hidden mutations within the genome that are known to shape variation in complex traits (Fraser and Xie 2009; Eichler *et al.* 2010; Chakraborty *et al.* 2019), and therefore identifying them is a critical step in dissecting complex traits. We found 4 SVs that fall within Q5 (Supplementary Table 4), including an insertion within *anxB9*, that occurs in the founder A3 haplotype. Interestingly, the A3 founder has one of the lower incapacitation scores (Fig. 3c) at Q5. Within all 7 QTLs, we found a total of 413 SVs (Supplementary Table 3). Lastly, we performed a manual search on FlyBase (Gramates *et al.* 2022) to investigate previous findings of these genes being implicated with thermal tolerance. Of the 5 genes we present, only very recently anxB9 has been shown to be slightly differently expressed in *D. melanogaster* larva after exposure to cold stress (Freda *et al.* 2022). The other 4 genes have not been shown to have direct implications for thermal tolerance previously. Thus, our results showing both differential expression in low and high-performing cohorts and a consistent effect following RNAi knockdown of these same genes within a large effect QTL are the first suggestion that these genes may be involved in thermal tolerance.

Discussion

We identified 7 genomic regions that influence thermal tolerance in the DSPR, including 1 large effect locus on chromosome 3R. We also identified multiple differentially expressed genes between cohorts that differ in high vs low thermal tolerance. For our most significant QTL, we integrated our RNA-seq findings and RNAi results to identify several candidate genes with multiple lines of evidence for their involvement in thermal tolerance. Overall, we found evidence for multiple potential causative variants within the large effect locus on Q5, supporting the hypothesis that in some cases, mapped QTLs do not represent a single causative variant, but instead a collection of variants acting in concert.

Thermal tolerance and its genetic basis have been investigated extensively previously, especially in the *D. melanogaster* model, providing the opportunity to compare our results to previously obtained results. However, a caveat is that there is no single method for assaying thermal tolerance, which both limits direct comparison in some cases, and highlights the fact that a different assay would very likely yield different results. The most common methods for assaying thermal tolerance include single extreme temperature assays (e.g. knockdown time assays) and ramping temperature assays (Sørensen *et al.* 2013). These are employed both for naive individuals, and for those exposed previously to

Table 2. Effect estimates and P-values from post hoc tests for each RNAi cross in our candidate list.

Gene	RNAi ID	Cross type	Effect estimate	P-value
AnxB9	38523	All cells	−34.6	0.42
	38523	Neurons	−28.2	0.72
	58111	All cells	−59.2	0.003
	58111	Neurons	−50.3	0.01
Cortactin	32871	All cells	−25.5	0.74
	32871	Neurons	5.9	1
	44425	All cells	−52.0	0.02
	44425	Neurons	−58.4	0.002
Dhc93AB	51511	All cells	−7.5	1
	51511	Neurons	−34.5	0.40
Mvl	55316	All cells	−21.1	0.98
	55316	Neurons	−96.3	1.24×10^{-9}
CG31207	60074	All cells	−25.0	0.89
	60074	Neurons	−70.1	8.42×10^{-5}

variable temperatures for variable times or at different stages, with some studies finding evidence for a different genetic basis for thermal tolerance at different life stages (e.g. Freda *et al.* 2017, 2019, 2022). In addition, most often survival is assayed but other phenotypes such as fertility (e.g. van Heerwaarden and Sgró 2021) have also been assayed. In addition, different rearing conditions used in different laboratories may also cause differences in results and limit the ability to make direct comparisons. For example, in our own experiment we maintained stock lines at 18°C before moving stocks to 25°C for testing in the F1 generation. This cold exposure could have intergenerational effects that are specific to our study. Nevertheless, it is essential to observe if there might be common loci identified in these different studies. Our results expand on previous studies that took genome-wide approaches to investigate the genetic basis of thermal tolerance in *D. melanogaster* (Norry *et al.* 2004, Norry, Gomez, *et al.* 2007; Norry, Sambucetti, *et al.* 2007, Norry *et al.* 2008; Morgan and Mackay 2006; Rand *et al.* 2010; Rolandi *et al.* 2018). We first compared our QTL dataset to Norry *et al.* (2008), because they characterized thermal tolerance in 2 divergent populations that were measured for thermal tolerance in both males and females. Norry *et al.* (2008) used heat-hardening measurements (exposure to high temps repeatedly) with an exposure temperature similar to our measurements. We found that our Q2 had an overlap with the data that was presented in that study, however, when we compared to the list of candidate genes only *Hsp23* was common among the 2 groups. This is not surprising because Frydenberg *et al.* (2003) performed genomic analysis on isofemale lines with a specific focus on *Hsp23*, *Hsp26*, and *Hsp27*, and found that at *Hsp23*, allele frequency differs across latitude clines in *D. melanogaster*. Interestingly, both the founding parents from DSPR—which we used in this study—and the RILs used in Norry *et al.* (2008) were collected in different latitudinal climatic locations, and represent different sets of genotypes, which could also contribute to the differences in the studies. We also compared our study to the findings of Rolandi *et al.* (2018). This group studied the genetic basis of thermal tolerance by measuring the upper thermal limits of 34 lines from the DGRP and performed GWAS to identify QTLs. The DGRP—like the DSPR—is one of the multiparental populations in fruit flies. Briefly, they reported 8 major SNPs that are associated with upper thermal limits in both males and females. We did not find any overlap between the SNPs they identified as candidates and our QTLs, nor did they correspond with genes that were significantly expressed within our QTLs. We also cross-referenced the candidate genes found in Norry *et al.* (2008) and Rolandi *et al.* (2018) to our list of genes that were significant between high and low thermal tolerance pools and found only 1 overlap—*Hsp23* (Norry *et al.* 2008). We have not directly compared effect estimates for the loci identified in these previous studies and our own, thus, loci we did not identify in this study may still be consistent with those findings and not identified in our study due to power. Thus, while this comparison to previous work does not allow us to make conclusions about differences in the genetic basis of thermal tolerance in these different study populations, this comparison does show that we have identified a set of novel QTLs and candidate genes that potentially influence thermal tolerance in the *D. melanogaster*, adding to our knowledge about the genetic basis of this critical trait.

Our findings emphasize the natural phenotypic and genetic variations in thermal tolerance (Sørensen *et al.* 2001, 2019; Norry *et al.* 2004, 2008; Overgaard and Sørensen 2008; Overgaard *et al.* 2011; Rolandi *et al.* 2018; MacLean, Sørensen, *et al.* 2019, MacLean, Overgaard, *et al.* 2019). This approach contrasts with a mutagenesis approach, which, while powerful, does not focus on natural genetic variation that is segregating. For example, we did not identify any *Hsp70* genes in our integrated approach comparing high and low thermal tolerance groups. This gene family has been well-established as having a role in heat tolerance, which stems from much of the earlier work done on elucidating mechanisms of thermal tolerance (Welte *et al.* 1993; Feder *et al.* 1996). However, more recent work by Jensen *et al.* (2010) suggests that *Hsp70* is not related to heat tolerance variation in adult *D. melanogaster*. Additionally, a GWAS study by Lecheta *et al.* (2020) also did not identify any *hsp* genes in their findings. The only gene from the *Hsp* family that was significantly differentially expressed within our design is *Hsp23*, within our pool treatment. Another potential reason for the lack of *Hsp70* genes in our study could be that most of the studies that identified *Hsp70* using *D. melanogaster* had a longer exposure or repeated exposure (Norry *et al.* 2008; Rampino *et al.* 2009; Cleves *et al.* 2020), whereas our measurement of thermal tolerance was a total of 10 min. Our focus on natural genetic variation is one of the advantages of the DSPR. In the DSPR system, the fly genome is unmodified (natural), however, we can rear them in the lab within a controlled environment, therefore reducing possible uncontrollable confounding effects. This approach allows for unbiased genomic scans to uncover natural segregating variants that would likely not be identified using single-gene approaches. Because of this systematic approach, we can identify multiple genome loci that influence complex traits, like thermal tolerance.

Genome scans are often paired with RNA-seq to further dissect the genetic basis of complex traits. We integrated RNA-seq to identify differentially expressed genes between high and low thermal tolerance cohorts within our 7 QTL regions (Wayne and McIntyre 2002). This integration continues to be a powerful approach used to narrow down potential candidate genes within QTLs that affect complex traits. We compared both low and high (baseline at room temp) groups and incubated vs room temp for genome-wide expression. This approach allowed us to identify a large set of genes whose expression differs constitutively among high and low thermal tolerant lines and the set of genes with expression changes following exposure to high temperatures. This rich dataset complements our QTL mapping results, giving additional information about the connection between gene expression and thermal tolerance. Often, the resolution of mapping approaches presents a challenge, with tens to hundreds of genes located within an associated QTL. For example, there are 472 genes located within the BCI of Q7 for the high and low cohorts, however, through RNA-seq, we were able to narrow down this list to 66 candidate genes. Notably, we might be excluding potential coding variants with this approach, however, initially focusing on regulatory variants was the most feasible approach in this case. An important limitation of our study is that we selected the 7 high and 7 low RILs for RNA-seq after initially measuring 140 RILs. Unfortunately, after measuring an additional 601 RILs and improving the accuracy and objectivity of scoring incapacitation, RILs in the high and low cohorts do not completely represent the tails of the thermal tolerance distribution. In particular, a single RIL that was originally in the high pool has a final mean incapacitation score closer to the RILs in the low pool. One of the reasons for developing a code-based scoring of incapacitation based on our activity traces was because we noticed human subjectivity in scoring the traces by hand. For example, in some of the early scoring of individuals, incapacitation was scored at timepoints after 60 s of inactivity due to signals of later activity, which can represent seizure rather than controlled movement by the fly. We addressed this issue and created objective criteria and implemented all of our scoring via code after validating this method (see *Methods*). However, because we chose the RILs for our RNA-seq pools from the earliest scoring, the line means were different from the final dataset with improved scoring. Despite this limitation, the high and low pools remain enriched for high vs low thermal tolerance lines (Fig. 1a). Furthermore, work done by Nielsen *et al.* (2006) suggests that phototransduction genes—mainly expressed in the eyes of flies—are upregulated in flies selected for increased heat tolerance, and because we used whole heads for the RNA-seq experiment, we wanted to rule out any possible phototransduction genes. We briefly compared our gene list from Q5 to their findings and found no commonality between the lists, which suggests that most of the genes we present to be candidate genes of thermal tolerance are not upregulated due to direct phototransduction activity, as described by Nielsen *et al.* (2006).

To functionally validate the QTL, we used the TRIP resource (Perkins *et al.* 2015), which is a powerful resource that provides the ability to screen more than 71% of the genes in the fly genome, because there is a mutant line for almost all the genes. We took advantage of this resource and ordered lines with gene disruption for the genes that fall within our Q5 region. In total, we screened 20 lines that we crossed to 2 pan-neuronal (*elavGAL4*) fly lines and 1 ubiquitously expressed line (*act-Gal4*). We then measured thermal tolerance in those lines together with background controls to identify how the reduction in the expression of our candidate genes influenced thermal tolerance. As hypothesized, we were not able to identify a single causal gene for thermal tolerance, but instead, our results are consistent with several genes contributing to the phenotype (Fig. 5). In fact, recent work by Herrmann and Yampolsky (2021) suggests that approximately 2,000 genes (1/8 of the Drosophila genome) either directly or indirectly contribute to temperature adaptation, suggesting a highly polygenic architecture with most variants having small effects and likely involving complex epistatic interactions (reviewed in Mackay 2015). This high complexity poses an obvious challenge and potential limit to our ability to validate all genes involved in thermal tolerance, and other highly complex traits.

Here, we present evidence for some of the genes we found to be influencing thermal tolerance, though the other genes within the QTL interval should not be discounted at this point. We highlight 5 lines that we consider to show interesting patterns. Those lines had a knockdown expression of *anxB9*, *cortactin*, *Dhc93AB*, *Mvl*, and *CG31207*. Based on a FlyBase and brief literature search, none of these 5 genes have been previously shown to directly influence thermal tolerance in adult *D. melanogaster*. In fact, relatively little is known about these genes. Briefly, *anxB9* is shown to be involved in the biological processes described in transportation, localization, and development, which is concluded based on work done mostly in mutants (Bejarano *et al.* 2008; Tjota *et al.* 2011). *Cortactin* is involved in cell organization and reproduction, in addition, to transport and development (Somogyi and Rørth 2004; Quinones *et al.* 2010; O'Connell *et al.* 2019), while *dhc93AB* is involved in nervous system processes, specifically sensory perception and movement (Gaudet *et al.* 2011; Senthilan *et al.* 2012). The gene *mvl* is shown to be involved in other nervous system processes and respond to stimuli, which were also inferred from *D. melanogaster* mutants (Orgad *et al.* 1998; Southon *et al.* 2008; Panda *et al.* 2013). Very little is known about *CG31207*, and thus our work presents some of the first phenotypic data to be associated with this gene.

Our study shows the challenges of identifying the genetic basis of highly polygenic traits even with a high powered design, an advanced QTL mapping panel, and multiple informative datasets. However, we have also demonstrated how we can gain insightful information from a multipronged approach, even if we do not identify "a single gene" associated with a particular QTL. Instead, taken together, our results are consistent with the hypothesis that there are multiple contributing variants within the large effect QTL we identify and additional contributing loci across the genome. Overall, our findings suggest a highly polygenic architecture for thermal tolerance, which may be characteristic of many complex traits, as has been suggested previously (Rockman 2012). This model of the genetic architecture of complex traits has a long history, from the infinitesimal model proposed by Fisher (1918), to the more recent omnigenic model developed from this foundation (Boyle *et al.* 2017). Future approaches to the investigation of the genetic mechanisms underlying thermal tolerance should recognize this inherent complexity and consider pulling in additional intermediate phenotypes and methods for assaying heat tolerance.

Data availability

Raw phenotypic data for measurements of thermal tolerance both in the heat box and heat plate, including the DeepLabCut models, are available from Zenodo (https://zenodo.org/record/7767713). RNA-seq data are available from the NCBI Short Read Archive (Leinonen *et al.* 2011) under SRA accession number: (https://www.ncbi.nlm.nih.gov/sra/SRR24828389). Raw re-sequencing data of the DSPR founder lines are deposited in the NCBI SRA under accession number SRA051316 and the RIL RAD genotyping data are available under accession number SRA051306. Founder genotype assignments from the hidden Markov model are available as 2 data packages in R (http://FlyRILs.org/). Additionally, see King, Merkes, *et al.* (2012) and Long *et al.* (2014) for more details on the DSPR datasets. The complete code used to perform all analyses is available on GitHub (https://github.com/EGKingLab/LearnMemTol).

Supplemental material available at GENETICS online.

Acknowledgments

This project was only possible due to the leadership and enthusiasm of Dr. Troy Zars, who sadly passed away in 2017. Troy dedicated his life to research, teaching, and mentorship, which is exhibited in his trainees and students. Troy had a passion for understanding the neurogenetics of learning and memory, and even after his passing his work still impacts the field, with ~1,200 citations from 2018 to present. Troy made an indelible mark, and his legacy and memory will forever be in the hearts of the many lives that he touched. Troy, we dedicate this paper to you! We thank the undergraduate researchers in Troy Zars lab, namely James Mrkvicka, Samuel Mitchell, and Christopher Posey, who helped with collecting preliminary data for this project. We also thank Dr. Stuart Macdonald for supplying us with the DSPR RILs and the Bloomington Stock Center for the TRiP lines (NIH/NIGMS, RO1-GM084947). Rapid Genomics (Gainesville, FL) conducted the RNA extractions, library prep, and readouts, and the University of Missouri Research Computing Support Services, in particular Christopher Bottoms and Jacob Gotberg, for their bioinformatics computing support. We also thank Paul Schmidt for comments on helping to improve this paper. In addition, we thank Jacelyn Shu (https://www.jacelyndesigns.com) for the experimental design figure.

Funding

This material is based upon work supported by the National Science Foundation under grant no. IOS-1654866 (TZ and EGK), National Institutes of Health R01GM117135 (EGK), Univerisyt of Missouri – MU Research Council grant URC-16-007 (TZ), National Institute of Health IMSD R25GM056901 (PAW-S), and Howard Hughes Medical Institute Gilliam Fellowship (PAW-S).

Conflicts of interest

The author(s) declare no conflicts of interest.

Literature cited

Angilletta MJ Jr. 2009. Thermal adaptation: a theoretical and empirical synthesis. Oxford: Oxford Academic. doi:10.1093/acprof.

Angilletta MJ, Hill T, Robson MA. 2002. Is physiological performance optimized by thermoregulatory behavior?: a case study of the eastern fence lizard, *Sceloporus undulatus*. J Therm Biol. 27(3): 199–204. doi:10.1016/S0306-4565(01)00084-5.

Angilletta MJ, Niewiarowski PH, Navas CA. 2002. The evolution of thermal physiology in ectotherms. J Therm Biol. 27(4):249–268. doi:10.1016/S0306-4565(01)00094-8.

Anttila K, Dhillon RS, Boulding EG, Farrell AP, Glebe BD, Elliott JAK, Wolters WR, Schulte PM. 2013. Variation in temperature tolerance among families of Atlantic salmon (*Salmo salar*) is associated with hypoxia tolerance, ventricle size and myoglobin level. J Exp Biol. 216(7):1183–1190. doi:10.1242/jeb.080556.

Bejarano F, Luque CM, Herranz H, Sorrosal G, Rafel N, Pham TT, Milán M. 2008. A gain-of-function suppressor screen for genes involved in dorsal–ventral boundary formation in the Drosophila wing. Genetics. 178(1):307–323. doi:10.1534/genetics.107.081869.

Bergland AO, Behrman EL, O'Brien KR, Schmidt PS, Petrov DA. 2014. Genomic evidence of rapid and stable adaptive oscillations over seasonal time scales in Drosophila. PLoS Genet. 10(11): e1004775. doi:10.1371/journal.pgen.1004775.

Boyle EA, Li YI, Pritchard JK. 2017. An expanded view of complex traits: from polygenic to omnigenic. Cell. 169(7):1177–1186. doi: 10.1016/j.cell.2017.05.038.

Bozinovic F, Medina NR, Alruiz JM, Cavieres G, Sabat P. 2016. Thermal tolerance and survival responses to scenarios of experimental climatic change: changing thermal variability reduces the heat and cold tolerance in a fly. J Comp Physiol B. 186(5):581–587. doi:10.1007/s00360-016-0980-6.

Bradski G. 2000. The OpenCV library. Dr Dobb's J: Softw Tools Professional Program. 25:120–123. doi:10.4236/oalib.1108286.

Broman KW, Sen S. 2009. A Guide to QTL Mapping with R/qtl. New York: Springer. p. 1–399.

Chakraborty M, Emerson JJ, Macdonald SJ, Long AD. 2019. Structural variants exhibit widespread allelic heterogeneity and shape variation in complex traits. Nat Commun. 10(1):4872. doi:10.1038/s41467-019-12884-1.

Chakraborty M, VanKuren NW, Zhao R, Zhang X, Kalsow S, Emerson JJ. 2018. Hidden genetic variation shapes the structure of functional elements in Drosophila. Nat Genet. 50(1):20–25. doi:10.1038/s41588-017-0010-y.

Cheruiyot EK, Haile-Mariam M, Cocks BG, MacLeod IM, Xiang R, Pryce JE. 2021. New loci and neuronal pathways for resilience to heat stress in cattle. Sci Rep. 11(1):16619. doi:10.1038/s41598-021-95816-8.

Churchill GA, Doerge RW. 1994. Empirical threshold values for quantitative trait mapping. Genetics. 138(3):963–971. doi:10.1093/genetics/138.3.963.

Cleves PA, Tinoco AI, Bradford J, Perrin D, Bay LK., Pringle JR. 2020. Reduced thermal tolerance in a coral carrying CRISPR-induced mutations in the gene for a heat-shock transcription factor. Proc Natl Acad Sci U S A. 117(46):28899–28905. doi:10.1073/pnas.1920779117.

Cubillos FA, Brice C, Molinet J, Tisné S, Abarca V, Tapia SM, Oporto C, García V, Liti G, Martínez C. 2017. Identification of nitrogen consumption genetic variants in yeast through QTL mapping and bulk segregant RNA-seq analyses. G3 (Bethesda). 7(6): 1693–1705. doi:10.1534/g3.117.042127

Díaz-Ricaurte JC, Serrano FC, Guevara-Molina EC, Araujo C, Martins M. 2021. Correction: does behavioral thermal tolerance predict distribution pattern and habitat use in two sympatric neotropical frogs? PLoS One. 16(2):e0246851. doi:10.1371/journal.pone.0246851.

Ding Y, Berrocal A, Morita T, Longden KD, Stern DL. 2016. Natural courtship song variation caused by an intronic retroelement in an ion channel gene. Nature. 536(7616):329–332. doi:10.1038/nature19093.

Dixon GB, Davies SW, Aglyamova GV, Meyer E, Bay LK, Matz MV. 2015. Genomic determinants of coral heat tolerance across latitudes. Science. 348(6242):1460–1462. doi:10.1126/science.1261224.

Dowd WW, King FA, Denny MW. 2015. Thermal variation, thermal extremes and the physiological performance of individuals. J Exp Biol. 218(12):1956–1967. doi:10.1242/jeb.114926.

DuRant SE, Hopkins WA, Carter AW, Stachowiak CM, Hepp GR. 2013. Incubation conditions are more important in determining early thermoregulatory ability than posthatch resource conditions in a precocial bird. Physiol Biochem Zool. 86(4):410–420. doi:10.1086/671128.

DuRant SE, Hopkins WA, Wilson AF, Hepp GR. 2012. Incubation temperature affects the metabolic cost of thermoregulation in a young precocial bird. Funct Ecol. 26(2):416–422. doi:10.1111/j.1365-2435.2011.01945.x.

Eichler EE, Flint J, Gibson G, Kong A, Leal SM, Moore JH, Nadeau JH. 2010. Missing heritability and strategies for finding the underlying causes of complex disease. Nat Rev Genet. 11(6):446–450. doi:10.1038/nrg2809.

Everett MV, Seeb JE. 2014. Detection and mapping of QTL for temperature tolerance and body size in Chinook salmon (*Oncorhynchus tshawytscha*) using genotyping by sequencing. Evol Appl. 7(4):480–492. doi:10.1111/eva.12147.

Fangue NA, Hofmeister M, Schulte PM. 2006. Intraspecific variation in thermal tolerance and heat shock protein gene expression in common killifish, *Fundulus heteroclitus*. J Exp Biol. 209(15): 2859–2872. doi:10.1242/jeb.02260.

Feder ME, Cartaño NV, Milos L, Krebs RA, Lindquist SL. 1996. Effect of engineering *Hsp70* copy number on *Hsp70* expression and tolerance of ecologically relevant heat shock in larvae and pupae of *Drosophila melanogaster*. J Exp Biol. 199(Pt 8):1837–1844. doi:10.1242/jeb.199.8.1837.

Fisher RA. 1918. The correlation between relatives on the supposition of Mendelian inheritance. Trans R Soc Edinb. 52(2):399–433. doi:10.1017/S0080456800012163.

Fraser HB, Xie X. 2009. Common polymorphic transcript variation in human disease. Genome Res. 19(4):567–575. doi:10.1101/gr.083477.108.

Frazer KA, Murray SS, Schork NJ, Topol EJ. 2009. Human genetic variation and its contribution to complex traits. Nat Rev Genet. 10(4): 241–251. doi:10.1038/nrg2554.

Frazier MR, Huey RB, Berrigan D. 2006. Thermodynamics constrains the evolution of insect population growth rates: "warmer is better." Am Nat. 168(4):512–520. doi:10.1086/506977.

Freda PJ, Alex JT, Morgan TJ, Ragland GJ. 2017. Genetic decoupling of thermal hardiness across metamorphosis in *Drosophila melanogaster*. Integr Comp Biol. 57(5):999–1009. doi:10.1093/icb/icx102.

Freda PJ, Ali ZM, Heter N, Ragland GJ, Morgan TJ. 2019. Stage-specific genotype-by-environment interactions for cold and heat hardiness in *Drosophila melanogaster*. Heredity (Edinb). 123(4):479–491. doi:10.1038/s41437-019-0236-9.

Freda PJ, Toxopeus J, Dowle EJ, Ali ZM, Heter N, Collier RL, Sower I, Tucker JC, Morgan TJ, Ragland GJ. 2022. Transcriptomic and functional genetic evidence for distinct ecophysiological responses across complex life cycle stages. J Exp Biol. 225(11):jeb244063. doi:10.1242/jeb.244063.

Frydenberg J, Hoffmann AA, Loeschcke V. 2003. DNA sequence variation and latitudinal associations in *hsp23*, *hsp26* and *hsp27* from natural populations of *Drosophila melanogaster*. Mol Ecol. 12(8): 2025–2032. doi:10.1046/j.1365-294X.2002.01882.x.

Gaspar P, Arif S, Sumner-Rooney L, Kittelmann M, Bodey AJ, Stern DL, Nunes MDS, McGregor AP. 2020. Characterization of the genetic architecture underlying eye size variation within *Drosophila melanogaster* and *Drosophila simulans*. G3 (Bethesda): Genes, Genomes, Genetics. 10(3):1005–1018. doi:10.1534/g3.119.400877.

Gaudet P, Livstone MS, Lewis SE, Thomas PD. 2011. Phylogenetic-based propagation of functional annotations within the Gene Ontology consortium. Brief Bioinform. 12(5): 449–462. doi:10.1093/bib/bbr042.

Gramates LS, Agapite J, Attrill H, Calvi BR, Crosby MA, dos Santos G, Goodman JL Goutte-Gattat D, Jenkins VK, Kaufman T, *et al.* 2022. FlyBase: a guided tour of highlighted features. Genetics. 220(4): iyac035. doi:10.1093/genetics/iyac035.

Grinder RM, Bassar RD, Auer SK. 2020. Upper thermal limits are repeatable in Trinidadian guppies. J Therm Biol. 90:102597. doi:10.1016/j.jtherbio.2020.102597.

Gunderson AR, Stillman JH. 2015. Plasticity in thermal tolerance has limited potential to buffer ectotherms from global warming. Proc Biol Sci. 282(1808):20150401. doi:10.1098/rspb.2015.0401.

Haley CS, Knott SA. 1992. A simple regression method for mapping quantitative trait loci in line crosses using flanking markers. Heredity (Edinb). 69(4):315–324. doi:10.1038/hdy.1992.131.

Herrmann M, Yampolsky LY. 2021. False and true positives in arthropod thermal adaptation candidate gene lists. Genetica. 149(3): 143–153. doi:10.1007/s10709-021-00122-w.

Highfill CA, Tran JH, Nguyen SKT, Moldenhauer TR, Wang X, Macdonald SJ. 2017. Naturally segregating variation at *Ugt86Dd* contributes to nicotine resistance in *Drosophila melanogaster*. Genetics. 207(1):311–325. doi:10.1534/genetics.117.300058.

Hoffmann AA. 2010. Physiological climatic limits in *Drosophila*: patterns and implications. J Exp Biol. 213(6):870–880. doi:10.1242/jeb.037630.

Hoffmann AA, Sørensen JG, Loeschcke V. 2003. Adaptation of Drosophila to temperature extremes: bringing together quantitative and molecular approaches. J Therm Biol. 28(3):175–216. doi:10.1016/S0306-4565(02)00057-8.

Hoffmann AA, Turelli M, Simmons GM. 1986. Unidirectional incompatibility between populations of *Drosophila simulans*. Evolution. 40(4):692–701. doi:10.2307/2408456.

Hothorn T, Bretz F, Westfall P. 2008. Simultaneous inference in general parametric models. Biom J. 50(3):346–363. doi:10.1002/bimj.200810425.

Huey RB, Berrigan D. 2001. Temperature, demography, and ectotherm fitness. Am Nat. 158(2):204–210. doi:10.1086/321314.

James AC, Azevedo RB, Partridge L. 1997. Genetic and environmental responses to temperature of *Drosophila melanogaster* from a latitudinal cline. Genetics. 146(3):881–890. doi:10.1093/genetics/146.3.881.

Jensen LT, Cockerell FE, Kristensen TN, Rako L, Loeschcke V, McKechnie SW, Hoffmann AA. 2010. Adult heat tolerance variation in *Drosophila melanogaster* is not related to Hsp70 expression. J Exp Zool A Ecol Genet Physiol. 313A(1):35–44. doi:10.1002/jez.573.

Jørgensen LB, Malte H, Overgaard J. 2019. How to assess *Drosophila* heat tolerance: unifying static and dynamic tolerance assays to predict heat distribution limits. Funct Ecol. 33(4):629–642. doi:10.1111/1365-2435.13279.

Jørgensen LB, Robertson RM, Overgaard J. 2020. Neural dysfunction correlates with heat coma and CTmax in *Drosophila* but does not set the boundaries for heat stress survival. J Exp Biol. 223(13):jeb218750. doi:10.1242/jeb.218750.

Kim D, Langmead B, Salzberg SL. 2015. HISAT: a fast spliced aligner with low memory requirements. Nat Methods. 12(4):357. doi:10.1038/nmeth.3317.

Kim K-S, Seibert JT, Edea Z, Graves KL, Kim E-S, Keating AF, Baumgard LH, Ross JW, Rothschild MF. 2018. Characterization of the acute heat stress response in gilts: III. Genome-wide association studies of thermotolerance traits in pigs. J Anim Sci. 96(6): 2074–2085. doi:10.1093/jas/sky131.

King EG, Macdonald SJ, Long AD. 2012. Properties and power of the Drosophila Synthetic Population Resource for the routine dissection of complex traits. Genetics. 191(3):935–949. doi:10.1534/genetics.112.138537.

King EG, Merkes CM, McNeil CL, Hoofer SR, Sen S, Broman KW, Long AD, Macdonald SJ. 2012. Genetic dissection of a model complex trait using the *Drosophila* Synthetic Population Resource. Genome Res. 22(8):1558–1566. doi:10.1101/gr.134031.111.

Krishnan M, Nguyen HT, Burke JJ. 1989. Heat shock protein synthesis and thermal tolerance in wheat. Plant Physiol. 90(1):140–145. doi:10.1104/pp.90.1.140.

Kristensen TN, Hoffmann AA, Overgaard J, Sørensen JG, Hallas R, Loeschcke V. 2008. Costs and benefits of cold acclimation in field-released *Drosophila*. Proc Natl Acad Sci U S A. 105(1): 216–221. doi:10.1073/pnas.0708074105.

Lecheta MC, Awde DN, O'Leary TS, Unfried LN, Jacobs NA, Whitlock MH, McCabe E, Powers B, Bora K, Waters JS, *et al.* 2020. Integrating GWAS and transcriptomics to identify the molecular underpinnings of thermal stress responses in *Drosophila melanogaster*. Front Genet. 11:658. doi:10.3389/fgene.2020.00658.

Leek JT, Johnson WE, Parker HS, Jaffe AE, Storey JD. 2012. The sva package for removing batch effects and other unwanted variation in high-throughput experiments. Bioinformatics. 28(6): 882–883. doi:10.1093/bioinformatics/bts034.

Leggett RM, Ramirez-Gonzalez RH, Clavijo BJ, Waite D, Davey RP. 2010. Sequencing quality assessment tools to enable data-driven informatics for high throughput genomics. Front Genet. 4:288. doi:10.3389/fgene.2013.00288.

Leinonen R, Sugawara H, Shumway M, International Nucleotide Sequence Database Collaboration. 2011. The sequence read archive. Nucleic Acids Res. 39(Database issue):D19–D21. doi:10.1093/nar/gkq1019.

Lockwood BL, Julick CR, Montooth KL. 2017. Maternal loading of a small heat shock protein increases embryo thermal tolerance in *Drosophila melanogaster*. J Exp Biol. 220(Pt 23):4492–4501. doi:10.1242/jeb.164848.

Long AD, Macdonald SJ, King EG. 2014. Dissecting complex traits using the Drosophila Synthetic Population Resource. Trends Genet. 30(11):488–495. doi:10.1016/j.tig.2014.07.009.

Love MI, Huber W, Anders S. 2014. Moderated estimation of fold change and dispersion for RNA-seq data with DESeq2. Genome Biol. 15(12):550. doi:10.1186/s13059-014-0550-8.

Machado HE, Bergland AO, Taylor R, Tilk S, Behrman E, Dyer K, Fabian DK, Flatt T, González J, Karasov TL, *et al.* 2021. Broad geographic sampling reveals the shared basis and environmental correlates of seasonal adaptation in *Drosophila*. Elife. 10:e67577. doi:10.7554/eLife.67577.

Mackay TFC. 2001. The genetic architecture of quantitative traits. Annu Rev Genet. 35(1):303–339. doi:10.1146/annurev.genet.35.102401.090633.

Mackay TFC. 2015. Epistasis for quantitative traits in *Drosophila*. Methods Mol Biol. 1253: 47–70. doi:10.1007/978-1-4939-2155-3_4.

MacLean HJ, Overgaard J, Kristensen TN, Lyster C, Hessner L, Olsvig E, Sørensen JG. 2019. Temperature preference across life stages and acclimation temperatures investigated in four species of *Drosophila*. J Therm Biol. 86:102428. doi:10.1016/j.jtherbio.2019.102428.

MacLean HJ, Sørensen JG, Kristensen TN, Loeschcke V, Beedholm K, Kellermann V, Overgaard J. 2019. Evolution and plasticity of thermal performance: an analysis of variation in thermal tolerance and fitness in 22 *Drosophila* species. Philos Trans R Soc Lond B Biol Sci. 374(1778):20180548. doi:10.1098/rstb.2018.0548.

Manichaikul A, Dupuis J, Sen S, Broman KW. 2006. Poor performance of bootstrap confidence intervals for the location of a quantitative trait locus. Genetics. 174(1):481–489. doi:10.1534/genetics.106.061549.

Martin M. 2011. Cutadapt removes adapter sequences from high-throughput sequencing reads. EMBnet J. 17(1):10–12. doi:10.14806/ej.17.1.200.

Mathis A, Mamidanna P, Cury KM, Abe T, Murthy VN, Mathis MW, Bethge M. 2018. DeepLabCut: markerless pose estimation of user-defined body parts with deep learning. Nat Neurosci. 21(9): 1281–1289. doi:10.1038/s41593-018-0209-y.

Matz MV, Treml EA, Aglyamova GV, Bay LK. 2018. Potential and limits for rapid genetic adaptation to warming in a Great Barrier Reef coral. PLoS Genet. 14(4):e1007220. doi:10.1371/journal.pgen.1007220.

Morgan TJ, Mackay TFC. 2006. Quantitative trait loci for thermotolerance phenotypes in *Drosophila melanogaster*. Heredity (Edinb). 96(3):232–242. doi:10.1038/sj.hdy.6800786.

Nath T, Mathis A, Chen AC, Patel A, Bethge M, Mathis MW. 2019. Using DeepLabCut for 3D markerless pose estimation across species and behaviors. Nat Protoc. 14(7):2152–2176. doi:10.1038/s41596-019-0176-0.

Ng'oma E, Williams-Simon PA, Rahman A, King EG. 2020. Diverse biological processes coordinate the transcriptional response to nutritional changes in a *Drosophila melanogaster* multiparent population. BMC Genomics. 21(1):84. doi:10.1186/s12864-020-6467-6.

Nielsen MM, Sørensen JG, Kruhøffer M, Justesen J, Loeschcke V. 2006. Phototransduction genes are up-regulated in a global gene expression study of *Drosophila melanogaster* selected for heat resistance. Cell Stress Chaperones. 11(4):325–333. doi:10.1379/CSC-207.1.

Nord A, Nilsson J-Å. 2011. Incubation temperature affects growth and energy metabolism in blue tit nestlings. Am Nat. 178(5): 639–651. doi:10.1086/662172.

Norry FM, Dahlgaard J, Loeschcke V. 2004. Quantitative trait loci affecting knockdown resistance to high temperature in *Drosophila melanogaster*. Mol Ecol. 13(11):3585–3594. doi:10.1111/j.1365-294X.2004.02323.x.

Norry FM, Gomez FH, Loeschcke V. 2007. Knockdown resistance to heat stress and slow recovery from chill coma are genetically associated in a quantitative trait locus region of chromosome 2 in *Drosophila melanogaster*. Mol Ecol. 16(15):3274–3284. doi:10.1111/j.1365-294X.2007.03335.x.

Norry FM, Sambucetti P, Scannapieco AC, Gomez FH, Loeschcke V. 2007. X-linked QTL for knockdown resistance to high temperature in *Drosophila melanogaster*. Insect Mol Biol. 16(4):509–513. doi:10.1111/j.1365-2583.2007.00747.x.

Norry FM, Scannapieco AC, Sambucetti P, Bertoli CI, Loeschcke V. 2008. QTL for the thermotolerance effect of heat hardening, knockdown resistance to heat and chill-coma recovery in an intercontinental set of recombinant inbred lines of *Drosophila melanogaster*. Mol Ecol. 17(20):4570–4581. doi:10.1111/j.1365-294X.2008.03945.x.

O'Connell ME, Sridharan D, Driscoll T, Krishnamurthy I, Perry WG, Applewhite DA. 2019. The *Drosophila* protein, nausicaa, regulates lamellipodial actin dynamics in a cortactin-dependent manner. Biol Open. 8(6):bio038232. doi:10.1242/bio.038232.

Orgad S, Nelson H, Segal D, Nelson N. 1998. Metal ions suppress the abnormal taste behavior of the *Drosophila* mutant *malvolio*. J Exp Biol. 201(1):115–120. doi:10.1242/jeb.201.1.115.

Ørsted M, Hoffmann AA, Rohde PD, Sørensen P, Kristensen TN. 2019. Strong impact of thermal environment on the quantitative genetic basis of a key stress tolerance trait. Heredity (Edinb). 122(3): 315–325. doi:10.1038/s41437-018-0117-7.

Ostrowski D, Salari A, Zars M, Zars T. 2018. A biphasic locomotor response to acute unsignaled high temperature exposure in *Drosophila*. PLoS One. 13(6):e0198702. doi:10.1371/journal.pone.0198702.

Overgaard J, Kristensen TN, Mitchell KA, Hoffmann AA. 2011. Thermal tolerance in widespread and tropical *Drosophila* species: does phenotypic plasticity increase with latitude? Am Nat. 178(S1):S80–S96. doi:10.1086/661780.

Overgaard J, Sørensen JG. 2008. Rapid thermal adaptation during field temperature variations in *Drosophila melanogaster*. Cryobiology. 56(2):159–162. doi:10.1016/j.cryobiol.2008.01.001.

Overgaard J, Tomcala A, Sørensen JG, Holmstrup M, Krogh PH, Šimek P, Koštál V. 2008. Effects of acclimation temperature on thermal tolerance and membrane phospholipid composition in the fruit fly *Drosophila melanogaster*. J Insect Physiol. 54(3):619–629. doi:10.1016/j.jinsphys.2007.12.011.

Panda D, Rose PP, Hanna SL, Gold B, Hopkins KC, Lyde RB, Marks MS, Cherry S. 2013. Genome-wide RNAi screen identifies SEC61A and VCP as conserved regulators of Sindbis virus entry. Cell Rep. 5(6): 1737–1748. doi:10.1016/j.celrep.2013.11.028.

Perkins LA, Holderbaum L, Tao R, Hu Y, Sopko R, McCall K, Yang-Zhou D, Flockhart I, Binari R, Shim H-S, *et al.* 2015. The transgenic RNAi

project at harvard medical school: resources and validation. Genetics. 201(3):843–852. doi:10.1534/genetics.115.180208.
Perry GML, Danzmann RG, Ferguson MM, Gibson JP. 2001. Quantitative trait loci for upper thermal tolerance inoutbred strains of rainbow trout (*Oncorhynchus mykiss*). Heredity (Edinb). 86(3):333–341. doi:10.1046/j.1365-2540.2001.00838.x.
Pertea M, Kim D, Pertea GM, Leek JT, Salzberg SL. 2016. Transcript-level expression analysis of RNA-seq experiments with HISAT, StringTie and Ballgown. Nat Protoc. 11(9): 1650–1667. doi:10.1038/nprot.2016.095.
Pertea M, Pertea GM, Antonescu CM, Chang T-C, Mendell JT, Salzberg SL. 2015. StringTie enables improved reconstruction of a transcriptome from RNA-seq reads. Nat Biotechnol. 33(3):290–295. doi:10.1038/nbt.3122.
Pinheiro JC, Bates DM. 2000. Mixed-Effects Models in S and S-PLUS. New York: Springer.
Pinheiro J, Bates D, R Core Team. 2023. nlme: Linear and nonlinear mixed effects models. https://cran.r-project.org/web/packages/nlme/nlme.pdf.
Pintanel P, Tejedo M, Ron SR, Llorente GA, Merino-Viteri A. 2019. Elevational and microclimatic drivers of thermal tolerance in andean *Pristimantis* frogs. J Biogeogr. 46(8): 1664–1675. doi:10.1111/jbi.13596.
Pörtner HO. 2002. Climate variations and the physiological basis of temperature dependent biogeography: systemic to molecular hierarchy of thermal tolerance in animals. Comp Biochem Physiol A Mol Integr Physiol. 132(4):739–761. doi:10.1016/S1095-6433(02)00045-4.
Posit team. 2023. RStudio: integrated development environment for R. https://www.r-project.org/conferences/useR-2011/abstracts/180111-allairejj.pdf.
Quinones GA, Jin J, Oro AE. 2010. I-BAR protein antagonism of endocytosis mediates directional sensing during guided cell migration. J Cell Biol. 189(2):353–367. doi:10.1083/jcb.200910136.
Rampino P, Mita G, Pataleo S, De Pascali M, Di Fonzo N, Perrotta C. 2009. Acquisition of thermotolerance and HSP gene expression in durum wheat (*Triticum durum* Desf.) cultivars. Environ Exp Bot. 66(2):257–264. doi:10.1016/j.envexpbot.2009.04.001.
Rand DM, Weinreich DM, Lerman D, Folk D, Gilchrist GW. 2010. Three selections are better than one: clinal variation of thermal QTL from independent selection experiments in Drosophila. Evolution. 64(10):2921–2934. doi:10.1111/j.1558-5646.2010.01039.x.
R Core Team. 2023. R: a language and environment for statistical computing. https://ropensci.org/blog/2021/11/16/how-to-cite-r-and-r-packages/.
Rockman MV. 2012. The QTN program and the alleles that matter for evolution: all that's gold does not glitter. Evolution. 66(1):1–17. doi:10.1111/j.1558-5646.2011.01486.x.
Roff DA. 2008. Comparing sire and dam estimates of heritability: jackknife and likelihood approaches. Heredity (Edinb). 100(1): 32–38. doi:10.1038/sj.hdy.6801048.
Roff DA, Preziosi R. 1994. The estimation of the genetic correlation: the use of the jackknife. Heredity (Edinb). 73(5):544–548. doi:10.1038/hdy.1994.153.
Rolandi C, Lighton JRB, de la Vega GJ, Schilman PE, Mensch J. 2018. Genetic variation for tolerance to high temperatures in a population of *Drosophila melanogaster*. Ecol Evol. 8(21):10374–10383. doi:10.1002/ece3.4409.
Rudman SM, Greenblum SI, Rajpurohit S, Betancourt NJ, Hanna J, Tilk S, Yokoyama T, Petrov DA, Schmidt P. 2022. Direct observation of adaptive tracking on ecological time scales in *Drosophila*. Science. 375(6586):eabj7484. doi:10.1126/science.abj7484.
Schulte PM, Healy TM, Fangue NA. 2011. Thermal performance curves, phenotypic plasticity, and the time scales of temperature exposure. Integr Comp Biol. 51(5):691–702. doi:10.1093/icb/icr097.
Senthilan PR, Piepenbrock D, Ovezmyradov G, Nadrowski B, Bechstedt S, Pauls S, Winkler M, Möbius W, Howard J, Göpfert MC. 2012. Drosophila auditory organ genes and genetic hearing defects. Cell. 150(5):1042–1054. doi:10.1016/j.cell.2012.06.043.
Somogyi K, Rørth P. 2004. Cortactin modulates cell migration and ring canal morphogenesis during Drosophila oogenesis. Mech Dev. 121(1):57–64. doi:10.1016/j.mod.2003.10.003.
Sørensen JG, Dahlgaard J, Loeschcke V. 2001. Genetic variation in thermal tolerance among natural populations of *Drosophila buzzatii*: down regulation of Hsp70 expression and variation in heat stress resistance traits. Funct Ecol. 15(3):289–296. doi:10.1046/j.1365-2435.2001.00525.x.
Sørensen JG, Giribets MP, Tarrío R, Rodríguez-Trelles F, Schou MF, Loeschcke V. 2019. Expression of thermal tolerance genes in two *Drosophila* species with different acclimation capacities. J Therm Biol. 84:200–207. doi:10.1016/j.jtherbio.2019.07.005.
Sørensen JG, Loeschcke V, Kristensen TN. 2013. Cellular damage as induced by high temperature is dependent on rate of temperature change—investigating consequences of ramping rates on molecular and organismal phenotypes in *Drosophila melanogaster* Meigen 1830. J Exp Biol. 216(Pt 5):809–814. doi:10.1242/jeb.076356.
Southon A, Farlow A, Norgate M, Burke R, Camakaris J. 2008. Malvolio is a copper transporter in *Drosophila melanogaster*. J Exp Biol. 211(5):709–716. doi:10.1242/jeb.014159.
Sunday JM, Bates AE, Dulvy NK. 2011. Global analysis of thermal tolerance and latitude in ectotherms. Proc Biol Sci. 278(1713): 1823–1830. doi:10.1098/rspb.2010.1295.
Sunday JM, Bates AE, Dulvy NK. 2012. Thermal tolerance and the global redistribution of animals. Nat Clim Chang. 2(9):686–690. doi:10.1038/nclimate1539.
Tjota M, Lee S-K, Wu J, Williams JA, Khanna MR, Thomas CM. 2011. Annexin B9 binds to βH-spectrin and is required for multivesicular body function in *Drosophila*. J Cell Sci. 124(17):2914–2926. doi:10.1242/jcs.078667.
van Heerwaarden B, Sgró CM. 2021. Male fertility thermal limits predict vulnerability to climate warming. Nat Commun. 12(1):2214. doi:10.1038/s41467-021-22546-w.
Van Rossum G, Drake FL. 2009. Python 3 Reference Manual. Scotts Valley (CA): CreateSpace.
Vermeulen CJ, Bijlsma R, Loeschcke V. 2008a. QTL mapping of inbreeding-related cold sensitivity and conditional lethality in *Drosophila melanogaster*. J Evol Biol. 21(5):1236–1244. doi:10.1111/j.1420-9101.2008.01572.x.
Vermeulen CJ, Bijlsma R, Loeschcke V. 2008b. A major QTL affects temperature sensitive adult lethality and inbreeding depression in life span in *Drosophila melanogaster*. BMC Evol Biol. 8(1):297. doi:10.1186/1471-2148-8-297.
Wayne ML, McIntyre LM. 2002. Combining mapping and arraying: an approach to candidate gene identification. Proc Natl Acad Sci. 99(23):14903–14906. doi:10.1073/pnas.222549199.
Welte MA, Tetrault JM, Dellavalle RP, Lindquist SL. 1993. A new method for manipulating transgenes: engineering heat tolerance in a complex, multicellular organism. Curr Biol. 3(12):842–853. doi:10.1016/0960-9822(93)90218-D.
Wen J, Jiang F, Weng Y, Sun M, Shi X, Zhou Y, Yu L, Wu Z. 2019. Identification of heat-tolerance QTLs and high-temperature stress-responsive genes through conventional QTL mapping, QTL-seq and RNA-seq in tomato. BMC Plant Biol. 19(1):398. doi:10.1186/s12870-019-2008-3.

Williams-Simon PA, Posey C, Mitchell S, Ng'oma E, Mrkvicka JA, Zars T, King EG. 2019. Multiple genetic loci affect place learning and memory performance in *Drosophila melanogaster*. Genes Brain Behav. 18(7):e12581. doi:10.1111/gbb.12581.

Wustmann G, Rein K, Wolf R, Heisenberg M. 1996. A new paradigm for operant conditioning of *Drosophila melanogaster*. J Comp Physiol A. 179(3):429–436. doi:10.1007/BF00194996.

Yu Y, Hill AP, McCormick DA. 2012. Warm body temperature facilitates energy efficient cortical action potentials. PLoS Comput Biol. 8(4):e1002456. doi:10.1371/journal.pcbi.1002456.

Zars T. 2001. Two thermosensors in Drosophila have different behavioral functions. J Comp Physiol A. 187(3):235–242. doi:10.1007/s003590100194.

Editor: J. Gleason